TRANSONIC FLOW OVER A NON-LIFTING, SLENDER BODY OF REVOLUTION

Thesis by

W. W. Royce

In Partial Fulfillment of the Requirements

For the Degree of

Doctor of Philosophy

California Institute of Technology
Pasadena, California
1959

ABSTRACT

Sonic flow past a non-lifting, slender body of revolution is investigated by the use of small disturbance theory. An approximation for the local Mach number distribution is used to linearize the transonic potential equation. Solutions for the velocity components, pressure distribution, and drag are obtained in terms of simple integrals involving the body geometry. An extension to other Mach numbers in the transonic range is given. The theoretical pressure distribution and drag are found to give good agreement with experimental data.

ACKNOWLEDGMENTS

The author wishes to express his sincere appreciation to Dr. Julian D. Cole for the suggestion of the problem and for his continuing guidance and encouragement during the progress of this work.

Miss Katherine Burford, Mrs. Nell Kindig and Mrs. Jewel Colbert all contributed to the preparation of this manuscript and the author wishes to express his thanks for their capable help.

The Douglas Aircraft Company, through its scholarship program, provided the author with considerable financial aid for which he is deeply grateful.

TABLE OF CONTENTS

1. INTRODUCTION

The analysis of transonic flow about wings and bodies presents a formidable mathematical problem. The aerodynamic phenomena are described in mathematical terms by a set of complex differential equations which must be simplified in order to obtain solutions. This can be accomplished by assuming that the body or wing introduces only small disturbances to a uniform free stream. Such a procedure is justified if the body or wing is sufficiently slender and if the viscous effects are disregarded. However, this method of simplification is not sufficient to reduce the equations to a completely tractable form. The potential equation obtained in this manner is necessarily non-linear and of mixed elliptic-hyperbolic type. The theoretical worker must continually cope with these two complicating features in analyzing transonic flow problems.

The complexity of the purely mathematical problem of transonic flow is a reflection of the equally complex physical structure. The important flow regimes and phenomena occurring about a slender body of revolution immersed in a Mach number one free stream are sketched in fig. 1. The complete flow field can be divided into several distinct regions; each having quite different physical properties and, hence, mathematically described by different equations. Starting upstream the flow initially decelerates to a subsonic velocity, continuing to do so until it encounters the body where it then accelerates, as the stream-lines divide around the body, to sonic velocity at the sonic line. In this region the flow is subsonic and described by an elliptic differential equation. The flow continues to accelerate past the sonic line reaching

maximum velocity just ahead of the shock wave. Aft of the sonic line and ahead of the shock wave the flow is supersonic and described by a hyperbolic differential equation. The downstream characteristic from the body intersecting the sonic line at infinity is indicated in the figure. The region bounded by this characteristic and the sonic line has some upstream influence since in this region all downstream characteristics eventually intersect the sonic line and can possibly interact with the subsonic regime. Aft of the limiting characteristic no interaction is possible.

After reaching maximum velocity, the flow decelerates to a subsonic velocity passing through a weak shock in the process. The flow continues to decelerate until it passes the body and then accelerates back to free stream conditions. The boundary layer and turbulent wake are included in the sketch to indicate the regions where viscous effects are dominant.

A brief survey of existing transonic methods clearly illustrates the difficulties imposed by the non-linear, mixed nature of the transonic potential equation.

Hodograph Methods

Hodograph methods have been studied extensively in the past and were the first to yield quantitative information about transonic flow over two dimensional shapes. The hodograph transformation transforms the two-dimensional non-linear potential equation in the physical plane into a linear equation in the hodograph plane. This exact linearization unfortunately complicates the problem in other important respects. The Jacobian of the transformation can and frequently does

vanish in the supersonic regime locally invalidating the entire process. Physically interesting solutions are commonly many valued in the hodograph plane. The boundary conditions are transformed only with great difficulty and often not at all. Principally because of these difficulties the limited number of analytic solutions obtained by this method are all restricted to two-dimensional shapes of extreme simplicity. As the geometry becomes more complex, it is necessary to resort to numerical methods. Here the dual nature (elliptic-hyperbolic) of the equations greatly complicates the numerical calculations.

Expansion Methods

If the subsonic, transonic, and supersonic potential equations, derived from small disturbance theory, are compared, it is evident that the linear terms in each are identical. This would suggest that an expansion technique based on either the linearized subsonic or supersonic potential equation as a first order approximation might be used to study transonic flow conditions. However, Cole and Messiter[1] have shown that in order to obtain a transonic flow it is necessary that the differential equation for the first approximation be the nonlinear transonic potential equation of mixed type. The subsonic part of the fluid is represented by the elliptic region, the supersonic part by the hyperbolic region. If the simpler, linearized solution of subsonic or supersonic theory is used as a first approximation, the higher order terms will only be asymptotic solutions for a high subsonic or low supersonic Mach number. The closeness of approach to Mach number one from either side may be made as small as desired by suitably decreasing the thickness parameter; however, the transonic limit will not be achieved even in the limit of zero thickness.

Linearization Methods

For the case of transonic flow about a non-lifting, slender body of revolution the potential equation is non-linear in both the physical plane and the hodograph plane so that the hodograph transformation leads to no essential improvement. An expansion technique also leads to no improvement since the non-linearity must be retained in the first approximation. An obvious alternative is to employ an additional assumption regarding the nature of the potential or its derivatives to reduce the equation to linear form by simplifying the non-linear terms. Such a procedure is justified if the linear terms are dominant (which is the case for transonic flow about a slender body in a close neighborhood of the body) and if it is possible to make an accurate guess as to the nature of the potential or its derivatives. If this approach can be carried out in a simple and general way the benefits to be gained are enormous. One needs only to compare the present status of subsonic and supersonic theory with transonic theory to see why linearity of the governing equations is necessary. The theory of subsonic and supersonic flow, based on a linear potential equation, is essentially complete. A general theory of transonic flow does not exist. The blame for such a state of affairs must be attributed to the non-linear term.

The method outlined in subsequent sections of this thesis is based on a linearization technique. Two other methods, similar in concept though not in detail, have appeared in the literature; the first by Oswatitsch and Keune[2], and the second by Spreiter and Alksne[3,4,5,6].

Oswatitsch and Keune investigated the problem of transonic flow around a non-lifting, slender, half-body of revolution (maximum thickness at the trailing edge). They reduced the non-linear transonic potential equation

$$\phi_{rr} + \frac{1}{r}\phi_r = (\gamma+1)\phi_x \phi_{xx} \quad *$$

to a linear form by assuming that ϕ_{xx} can be approximated by a constant to obtain

$$\phi_{rr} + \frac{1}{r}\phi_r = a^2 \phi_x .$$

This approximation is justified on the basis that in all of its important parts the flow is accelerating uniformly. The mixed form of the original equation has been lost in the approximation as the final equation is of parabolic type in the entire (x, r) plane. This latter condition leads to some difficulties in applying the upstream boundary condition because the solution to a parabolic equation can have no upstream influence. Thus, if the velocity disturbances at upstream infinity are set equal to zero they remain so all the way up to the plane containing the body nose and perpendicular to the body axis. The authors then show, by means of an auxiliary computation, that if the velocity disturbances are made to vanish in the transverse plane containing the nose point rather than at upstream infinity, the error introduced is at least an order of magnitude less than the final solutions for the disturbance velocity components.

---

* These equations are introduced here to clarify the ensuing discussion. The derivation of these equations and the notation is discussed in Section 2.

Computations based on the parabolic equation are actually carried out only in the subsonic region up to the sonic line. Although there is no reason to stop at the sonic line, the authors recommend using a characteristics method in the supersonic region.

The theoretical pressure distribution and drag are compared with experimental results obtained by Drougge[7]. The agreement is quite good except in a region on the aft part of the body where viscous effects are known to predominate. A particularly interesting result for the drag coefficient is obtained; namely, that the drag coefficient for a half-body is exactly half the value predicted by linearised supersonic slender body theory.

The technique proposed by Spreiter and Alksne is based on the premise that both ϕ_x and ϕ_{xx} are slowly varying functions of the coordinates. Hence, in the non-linear term, either may be approximated locally by a constant. If the flow is locally subsonic the transonic potential equation is replaced by

$$\phi_{rr} + \frac{1}{r}\phi_r = -\lambda_E \phi_{xx}$$

and if the flow is locally supersonic

$$\phi_{rr} + \frac{1}{r}\phi_r = \lambda_H \phi_{xx}.$$

If the flow is mixed and includes the sonic line the potential equation is approximated by

$$\phi_{rr} + \frac{1}{r}\phi_r - \lambda_P \phi_x = f_P.$$

Here

$$\lambda_E = 1 - M_\infty^2 - M_\infty^2 (\gamma+1)\phi_x$$

$$\lambda_H = M_\infty^2 - 1 + M_\infty^2 (\gamma+1)\phi_x$$

$$\lambda_P = M_\infty^2 (\gamma+1)\phi_{xx}$$

$$f_P = (M_\infty^2 - 1)\phi_{xx}.$$

These expressions follow directly from the transonic potential equation for a free stream Mach number close to one -

$$(1-M_\infty^2)\phi_{xx} + \phi_{rr} + \frac{1}{r}\phi_r = (\gamma+1)M_\infty^2 \phi_x \phi_{xx}.$$

In each case a solution for ϕ_x is obtained by solving the linearized form, treating λ_E , λ_H or λ_P as positive constants. The exact expressions for λ_E , λ_H and λ_P are reinserted into the linearized solutions to obtain ordinary, first order, non-linear differential equations of the form

$$\frac{d}{dx}(\phi_x) = F(x, \phi_x)$$

where the function, $F(x, \phi_x)$ differs between the elliptic, hyperbolic, or parabolic case. The resultant equations are solved by numerical methods using computing machines.

An extensive comparison with experiment and other theories is made. The agreement is excellent indicating the results obtained by this method are of surprisingly high quality. Although no direct

justification for the mathematical steps leading to the final solution is given, the excellent agreement with other known results amply justifies the method. In addition it is by far the simplest method yet devised for investigating transonic flow about arbitrary two and three dimensional shapes.

The methods of Oswatitsch and Keune, Spreiter and Alksne, and that to be outlined in the following sections of this thesis represent the first real steps toward a general theory of transonic flow about arbitrary shapes suitable for engineering applications.

2. METHOD OF SOLUTION

The method outlined in this study, like that of Oswatitsch and Keune, and Spreiter and Alksne, uses a special approximation to simplify the non-linear term in the transonic potential equation. However, unlike the latter two methods, here the solution is obtained from an equation of mixed elliptic-hyperbolic form. Both of these methods, first, divide the flow into elliptic, hyperbolic, and parabolic regions, solving each separately by the appropriate equation of fixed type, and then use a matching procedure on the common boundaries to join these separate solutions into a single continuous solution. No special matching procedure is required in the method given here. However, unlike that of Spreiter and Alksne, this method is restricted to slender bodies of revolution for which the dominant solution in the neighborhood of the body axis is known.

Mathematical Formulation

The following analysis solves for the pressure distribution and drag of a non-lifting, slender body of revolution in a uniform free stream of Mach number one. The exact non-viscous potential equation expressed in cylindrical polar coordinates can be simplified using the axial symmetry condition and the assumption of small disturbances about the free stream Mach number to obtain the approximate equation

$$\phi_{rr} + \frac{1}{r}\phi_r = (\gamma+1)\phi_x\phi_{xx} \qquad (1)$$

The exact equation is based on the principles of conservation of mass, momentum and energy throughout the flow. Since the flow is

uniform upstream and the rotation introduced by shocks is negligible for the slender, pointed body in transonic flow, it is possible to introduce a potential function.

The velocity components parallel and perpendicular to the free stream are related to the potential function, ϕ , by the equations

$$u = U(1+\phi_x) \tag{2a}$$

$$v = U\phi_r \tag{2b}$$

where U is the free stream velocity. All lengths have been made dimensionless by dividing by the body length.

The boundary conditions require that the velocities remain finite at infinity and that the flow is tangent to the body surface. Since it is assumed that $\phi_x \ll 1$, the boundary condition of tangent flow on the body becomes

$$\phi_r[x, \delta F(x)] = \delta F'(x) \quad *$$

where

$$\bar{r} = \delta F(x)$$

is the equation for the body surface, δ being the ratio of maximum thickness to length of the body. In this form the boundary condition on the body is too complicated to use and is inconsistent with the assumptions used to obtain the approximate transonic equation. Multiplying both sides of the equation by r and taking the limit as r goes to zero gives the slender body equivalent of the exact

---

* Here and elsewhere primes indicate differentiation with respect to the argument.

boundary condition,

$$\lim_{r \to 0} (r\phi_r) = \bar{r} \frac{d\bar{r}}{dx} . \tag{3}$$

The right hand side of equation 3 is just the source strength distribution.* Denoting the source strength distribution by $S(x)$, then

$$S(x) = \bar{r} \frac{d\bar{r}}{dx} . \tag{4}$$

The pressure coefficient based on free stream conditions is given by

$$C_p = -2\phi_x - \phi_r^2 . \tag{5}$$

In the analysis that follows, we need solve only for ϕ_x since the term, ϕ_r^2, evaluated on the body, is directly obtained from the boundary condition.

For the evaluation of the drag

$$\frac{D}{2\pi q_f} = \int_0^1 C_p S(x)\, dx \tag{6}$$

where q_f is the dynamic pressure based on free stream conditions.

The Approximation for the Non-Linear Term

It is easily seen that the dominant terms contributing to the solution of flow over a slender body of revolution in the neighborhood of the body are those involving derivatives with respect to r. If the non-linear term is ignored an asymptotic expansion, valid for r small, is easily obtained

$$\phi = f(x) \log r + g(x) + \cdots .$$

* See Appendix C.

$f(x)$ and $g(x)$ are arbitrary functions with respect to the differential equation which are determined from the boundary conditions. Specifically, $f(x)$ is determined from the inner boundary condition of tangent flow on the body.

$$\phi_r\Big|_{\text{boundary}} = \frac{f(x)}{\bar{r}} = \frac{d\bar{r}}{dx}$$

or

$$f(x) = S(x) .$$

$g(x)$ is determined from the outer boundary condition. For this purpose it is necessary to solve for the entire flow field retaining the terms in the differential equation involving derivatives with respect to X. Fortunately, this unwieldy procedure can be avoided by confining our attention to a neighborhood of the body. For this purpose a complete solution for $g(x)$ is not needed; we need only establish that $g(x)$ is of order δ^2.* Then it follows that in the neighborhood of the body

$$\phi \simeq S(x)\log r + g(x) + \cdots \simeq$$

$$\simeq S(x)\log\delta + \left[S(x)\log\frac{r}{\delta} + g(x)\right] + \cdots .$$

The first term is of order $\delta^2\log\delta$, the second term is of order δ^2 and is neglected.

This expression can be further simplified by expanding in a

* See Ref. 1

Taylor series

$$\phi=\left[S(\bar{x})+S''(\bar{x})\frac{(x-\bar{x})^2}{2}+S'''(\bar{x})\frac{(x-\bar{x})^3}{6}+\cdots\right]\log\delta$$

where $\bar{x}$ is defined by the equation

$$S'(\bar{x})=0.$$

Differentiating and retaining only the largest term near $x=\bar{x}$,

$$\phi_x=S''(\bar{x})(x-\bar{x})\log\delta. \tag{7}$$

The additional approximation is to linearize the transonic potential equation by replacing ϕ_x by the above expression.

Admittedly, the line of reasoning leading up to the approximation for ϕ_x is not strongly convincing. It is included only to provide a bare motivation for the approximation. The real justification for such a procedure is that it leads to the simplest equation that can be solved in closed form with any economy of effort and at the same time still retains the two important mathematical properties of the original differential equation; namely that (1) it changes mathematical form from an elliptic to a hyperbolic differential equation in a continuous fashion across the line, $x=\bar{x}$, which approximates the sonic line, and (2) it has the same dominant behavior in the neighborhood of the body axis.

The approximation corresponds, physically, to uniformly accelerating flow in the neighborhood of the body. From the body nose to some distance aft of the maximum thickness point the approximation is clearly justified. Ahead of the body the flow is decelerating

but conditions in this region will not appreciably influence pressures on the body. The flow will also be decelerating over most of the body aft of the maximum thickness point. In a limited region near the trailing edge of the body the assumed behavior of ϕ_x will be immaterial (presuming the correct order of magnitude is assumed) as the solution will be dependent only on the dominant linear terms. Thus, in a limited region aft of the maximum thickness point and forward of the trailing edge the approximation does not agree with the known behavior of the fluid. Since this region contributes a large portion of the drag, it would appear that the approximation might lead to serious error in predicting the drag. This is not the case, however, as the dominant terms result in a solution having the correct accelerating-decelerating property in spite of the approximation. If the geometry is limited to half-bodies, bodies having the maximum thickness near the trailing edge, ogive-cylinder combinations, or bodies of high fineness ratio the approximation should be completely valid since the decelerating region will either not exist or be completely unimportant.

It is convenient to redefine the origin of coordinates by letting

$$\bar{z} = x - \bar{x} \,. \tag{8}$$

The nose point $(x=0)$ will be denoted by $\bar{z}_0$, the trailing edge $(x=1)$ by $\bar{z}_1$. The source strength distribution $(S(x))$ in this transformed coordinate system will be denoted by $T(\bar{z})$. Finally, an acceleration constant is defined as follows:

$$a^2 = (\gamma+1)\, T'(0) \log \delta. \tag{9}$$

The governing equations then become

$$\phi_{rr} + \frac{1}{r}\phi_r = a^2 z \phi_{zz} \tag{10}$$

$$u = U(1 + \phi_z) \tag{11a}$$

$$v = U\phi_r \tag{11b}$$

$$\lim_{r \to 0}(r\phi_r) = T(z) \tag{12}$$

$$C_p = -2\phi_z - \phi_r^2 \tag{13}$$

$$\frac{D}{2\pi q_\infty} = \int_{z_0}^{z_1} C_p T(z)\, dz. \tag{14}$$

Characteristics in the Hyperbolic Regime

A general solution is obtained by distributing sources along the axis of the body in both the elliptic $(z<0)$ and hyperbolic $(z>0)$ regimes. Before carrying out the solution it is necessary to investigate the characteristic lines in the hyperbolic regime in order to determine the region of influence of the sources located in this regime. The differential equation for the characteristic directions is given by

$$\left(\frac{dr}{dz}\right)^2 = \frac{1}{a^2 z}. \tag{15}$$

The equations for the characteristics become

$$r - \frac{2}{a}\sqrt{z} = C_1 \tag{16a}$$

$$r + \frac{2}{a}\sqrt{z} = C_2. \tag{16b}$$

The characteristics take the form of a one-parameter family of parabolas tangent to the sonic line with the axis of the parabola parallel to the body axis. The characteristics are plotted in fig. 2.

A source located on the body axis at $z = \xi$ will have a region of influence within a semi-infinite volume of revolution generated by the parabola

$$\xi = \left(\sqrt{z} - \frac{ar}{2}\right)^2 .$$

Furthermore, conditions at a point (z, r) will be affected only by sources located on the axis such that

$$\xi \leq \left(\sqrt{z} - \frac{ar}{2}\right)^2 . \tag{17}$$

Source Solution for the Hyperbolic Regime

In this section the potential due to a source* of unit strength located on the body axis in the hyperbolic regime is determined. The differential equation takes the form

$$\phi_{rr} + \frac{1}{r}\phi_r - a^2 z \phi_{zz} = \frac{\delta(r)\,\delta(z-\xi)}{r} \tag{18}$$

Using the Hankel transform pair

$$\tilde{f}(\omega) = \int_0^\infty J_0(\omega r)\, f(r)\, r\, dr$$

$$f(r) = \int_0^\infty J_0(\omega r)\, \tilde{f}(\omega)\, \omega\, d\omega$$

---

* Here the term "source" is to be interpreted in the mathematical sense. Since the left hand side of equation 18 is approximately the continuity equation, it is evident that the mathematical source strength must be equal to the (dimensionless) fluid source strength in the slender body limit. This statement is verified in Appendix C.

the transformed equation becomes

$$\tilde{\phi}_{zz} + \frac{\omega^2}{a^2 z}\tilde{\phi} = -\frac{\delta(z-\zeta)}{a^2 z}.$$

The solution is obtained in terms of Bessel functions;

$$\tilde{\phi} = \begin{cases} A\sqrt{z}\,J_1\left(2\frac{\omega}{a}\sqrt{z}\right) + B\sqrt{z}\,Y_1\left(2\frac{\omega}{a}\sqrt{z}\right) & z > \zeta \\ 0 & z < \zeta \end{cases}$$

The potential must be zero for $z<\zeta$ as the source can have no upstream influence.

The constants A and B are determined from the conditions that

(i) $\tilde{\phi}$ is continuous at $z=\zeta$.

(ii) $\tilde{\phi}_z$ jumps by amount $-\frac{1}{a^2\zeta}$ at $z=\zeta$.

Using these conditions plus the Wronskian,

$$W\{J_0(y), Y_0(y)\} = \frac{2}{\pi y}$$

the transformed potential for $z>\zeta$ becomes

$$\tilde{\phi} = \frac{\pi\sqrt{z}}{a^2\sqrt{\zeta}}\left[Y_1\left(2\frac{\omega}{a}\sqrt{\zeta}\right)J_1\left(2\frac{\omega}{a}\sqrt{z}\right) - J_1\left(2\frac{\omega}{a}\sqrt{\zeta}\right)Y_1\left(2\frac{\omega}{a}\sqrt{z}\right)\right].$$

Substituting into the inversion integral

$$\phi = \begin{cases} \dfrac{\pi\sqrt{z}}{a^2\sqrt{\xi}}\displaystyle\int_0^\infty \left[Y_1\left(2\frac{\omega}{a}\sqrt{\xi}\right)J_1\left(2\frac{\omega}{a}\sqrt{z}\right) - J_1\left(2\frac{\omega}{a}\sqrt{\xi}\right)Y_1\left(2\frac{\omega}{a}\sqrt{z}\right)\right] J_0(\omega r)\,\omega\, d\omega & \sqrt{z} > \sqrt{\xi} + \frac{ar}{2} \\ 0 & \sqrt{z} < \sqrt{\xi} - \frac{ar}{2}. \end{cases} \tag{22}$$

The evaluation of this integral is given in Appendix A. The final result is

$$\phi_H = \begin{cases} -\dfrac{z + \xi - \frac{a^2r^2}{4}}{2\xi\sqrt{\left(z - \xi - \frac{a^2r^2}{4}\right)^2 - a^2r^2\xi}} & \sqrt{z} > \sqrt{\xi} + \frac{ar}{2} \\ 0 & \sqrt{z} < \sqrt{\xi} - \frac{ar}{2}. \end{cases} \tag{23}$$

The subscript, $(\ )_H$, has been added to denote the potential due to sources located in the hyperbolic regime.

In the neighborhood of the source the potential behaves like

$$\phi_H = -\frac{1}{\sqrt{(z-\xi)^2 - a^2 z r}}. \tag{24}$$

Locally, the influence of the potential decays like the inverse square root of the hyperbolic distance analogous to the behavior of the linearized supersonic source potential. These expressions would be identical (and also the differential equations for the potential) if $a^2 z$

were replaced by $(M_\infty^2 - 1)$. Actually in the approximation used here

$$a^2 z \simeq M_{local}^2 - 1. \tag{25}$$

This provides a close connection with the linearization method of Spreiter and Alksne for locally supersonic flow.

Source Solution for the Elliptic Regime

The analysis of the potential due to a unit-strength subsonic source follows along the same lines as that for the hyperbolic source.

Starting with the transformed differential equation

$$\tilde{\phi}_{zz} + \frac{\omega^2}{a^2 z}\tilde{\phi} = -\frac{\delta(z-\zeta)}{a^2 z}, \tag{19}$$

we have that

$$\tilde{\phi} = \begin{cases} A\sqrt{-z}\, I_1\left(2\frac{\omega}{a}\sqrt{-z}\right) + B\sqrt{-z}\, K_1\left(2\frac{\omega}{a}\sqrt{-z}\right) & z < \zeta \\ C\sqrt{-z}\, I_1\left(2\frac{\omega}{a}\sqrt{-z}\right) + D\sqrt{-z}\, K_1\left(2\frac{\omega}{a}\sqrt{-z}\right) & z > \zeta \end{cases} \tag{26}$$

The solution must have the following properties:

(i) $\tilde{\phi}$ is continuous at $z = \zeta$.

(ii) $\tilde{\phi}_z$ jumps by amount $-\frac{1}{a^2\zeta}$ at $z = \zeta$,

(iii) $\tilde{\phi}_z$ approaches zero as $z \to -\infty$,

(iv) $\tilde{\phi}_z$ is finite as $z \to 0$.

Using these conditions plus the Wronskian

$$W\{I_o(y), K_o(y)\} = -\frac{1}{y},$$

the transformed potential becomes

$$\phi = \begin{cases} -\frac{2\sqrt{-z}}{a^2\sqrt{-\xi}} I_1\left(2\frac{\omega}{a}\sqrt{-\xi}\right) K_1\left(2\frac{\omega}{a}\sqrt{-z}\right) & z < \xi \\ -\frac{2\sqrt{-z}}{a^2\sqrt{-\xi}} K_1\left(2\frac{\omega}{a}\sqrt{-\xi}\right) I_1\left(2\frac{\omega}{a}\sqrt{-z}\right) & z > \xi . \end{cases} \tag{27}$$

Substituting into the inversion integral

$$\phi = \begin{cases} -\frac{2\sqrt{-z}}{a^2\sqrt{-\xi}} \int_0^\infty I_1\left(2\frac{\omega}{a}\sqrt{-\xi}\right) K_1\left(2\frac{\omega}{a}\sqrt{-z}\right) J_o(\omega r)\, \omega\, d\omega & z < \xi \\ -\frac{2\sqrt{-z}}{a^2\sqrt{-\xi}} \int_0^\infty K_1\left(2\frac{\omega}{a}\sqrt{-\xi}\right) I_1\left(2\frac{\omega}{a}\sqrt{-z}\right) J_o(\omega r)\, \omega\, d\omega & z > \xi . \end{cases} \tag{28}$$

The evaluation of these integrals is given in Appendix B.

The final result is

$$\phi_E = -\frac{1}{4\xi} - \frac{z + \xi - \frac{a^2 r^2}{4}}{4\xi\sqrt{\left(z - \xi - \frac{a^2 r^2}{4}\right)^2 - a^2 r^2 \xi}} . \tag{29}$$

The subscript, $(\,)_E$, has been added to denote the potential due to sources located in the elliptic regime.

In the neighborhood of the source the potential becomes

$$\phi_E = -\frac{1}{4\xi} - \frac{1}{2\sqrt{(z-\xi)^2 - a^2 z r^2}} . \tag{30}$$

Since $\bar{z}$ is always negative the second term decays like the inverse square root of the elliptic distance analogous to the behavior of a subsonic source. The comments following equation 24 of the preceding Section also apply here.

Singular Behavior of the Integrated Solution

The velocity potential is obtained by integrating the product of the source strength distribution, $T(\xi)$, and the potential for a unit strength source over the sources within the domain of dependence of a point $(\bar{z}, r)$. In Appendix C it is shown that the boundary condition of tangent flow on the body is satisfied if the mathematical source strength is set equal to the fluid source strength, $T(\xi)$.

For $\bar{z} > \frac{a^2 r^2}{4}$ the potential becomes

$$\phi = -\frac{1}{4}\int_{z_0}^{0}\left[1 - \frac{\bar{z}+\xi-\frac{a^2r^2}{4}}{\sqrt{\left(\bar{z}-\xi-\frac{a^2r^2}{4}\right)^2 - a^2r^2\xi}}\right]\frac{T(\xi)}{\xi}\,d\xi + \tag{31}$$

$$-\frac{1}{2}\int_{z_0}^{\left(\sqrt{\bar{z}}-\frac{ar}{2}\right)^2}\left[\frac{\bar{z}+\xi-\frac{a^2r^2}{4}}{\sqrt{\left(\bar{z}-\xi-\frac{a^2r^2}{4}\right)^2 - a^2r^2\xi}}\right]\frac{T(\xi)}{\xi}\,d\xi .$$

For $\bar{z} < \frac{a^2 r^2}{4}$

$$\phi = -\frac{1}{4}\int_{z_0}^{0}\left[1 + \frac{\bar{z}+\xi-\frac{a^2r^2}{4}}{\sqrt{\left(\bar{z}-\xi-\frac{a^2r^2}{4}\right)^2 - a^2r^2\xi}}\right]\frac{T(\xi)}{\xi}\,d\xi . \tag{32}$$

The integrand of the second integral of equation 31 is singular at the origin and at the upper limit. Both singularities are integrable and cause no difficulty. However, the potential and its derivatives are singular on the characteristic from the origin, $z=\frac{a^2r^2}{4}$, whether approaching from the left (equation 32), or the right (equation 31). Thus the above representation for the potential cannot be a solution since it violates the regularity condition of no infinite velocities within the fluid.

The nature of this singularity in the potential is investigated in Appendix D. The singular part of the potential is found to be

$$\phi_{sing} = -\frac{1}{2} T(0) \log\left| z - \frac{a^2 r^2}{4} \right| \tag{33}$$

independent of the direction of approach. This singular behavior is somewhat surprising since it is usually associated with some discontinuity in body geometry which is not the case here.

To analyze the origin of this singularity, it is instructive to investigate the potential of a unit strength source as the source point approaches and passes through the origin from the left. If we approximate the unit-strength elliptic source potential (equation 30), and the hyperbolic source potential (equation 23), in the neighborhood

of the origin by a series expansion in ξ we obtain

$$\phi_E = \begin{cases} \left[-\frac{1}{2\xi} - \frac{z}{2\left(z-\frac{a^2r^2}{4}\right)^2} + \Theta(\xi)\right] T(\xi) & z > \frac{a^2r^2}{4} \quad (34a) \\ \left[\frac{z}{2\left(z-\frac{a^2r^2}{4}\right)^2} + \Theta(\xi)\right] T(\xi) & z < \frac{a^2r^2}{4} \quad (34b) \end{cases}$$

$$\phi_H = \begin{cases} \left[-\frac{1}{2\xi} - \frac{z}{\left(z-\frac{a^2r^2}{4}\right)^2} + \Theta(\xi)\right] T(\xi) & z > \frac{a^2r^2}{4} \quad (34c) \\ 0 & z < \frac{a^2r^2}{4} \quad (34d) \end{cases}$$

The apparently dominant term, $-\frac{T(\xi)}{2\xi}$, appearing in both ϕ_E and ϕ_H for $z > \frac{a^2r^2}{4}$ corresponds to the integrable singularity at the origin of the second integral of equation 31. Since this term contributes nothing to this integral in the neighborhood of the origin, it may be disregarded here.

For a fixed point (z,r) such that $z > \frac{a^2r^2}{4}$ there is a jump in the potential from $-\frac{z}{2\left(z-\frac{a^2r^2}{4}\right)^2}$ to $-\frac{z}{\left(z-\frac{a^2r^2}{4}\right)^2}$ as the source passes through the origin. Thus, even though the source strength is constant, the effect of the source is doubled as it moves into the hyperbolic regime. This is in agreement with the well known property of fluid sources, namely that a supersonic source is twice as effective as a subsonic source of equal strength.

For a fixed point (z,r) such that $z < \frac{a^2r^2}{4}$ the potential jumps from $\frac{z}{2\left(z-\frac{a^2r^2}{4}\right)^2}$ to zero as the source passes through the origin. In either case this discontinuous behavior at the origin creates a

singularity which is propagated along the limiting characteristic from the origin.

The solution for a single finite source of any order located at the origin can be easily determined using similarity to reduce the number of independent variables. In Appendix E two such solutions are carried out; the first corresponding to an ordinary source at the origin, and the second corresponding to a source distribution having a finite jump in strength at the origin. The first is shown to have the same functional form as the unit strength hyperbolic or elliptic source at the origin (equation 34). The second has the same form as the singular part of the potential on the characteristic, $z=\frac{a^2R^2}{4}$.

The Complete Solution

The singularity on the characteristic, $z=\frac{a^2R^2}{4}$, must be removed in order to satisfy the regularity condition of no infinite velocities in the fluid. The interpretation of this procedure is that the flow cannot be represented simply as a line of sources of the type constructed; an extra solution must be added to fix up the singularity. This extra solution is analogous to the solutions used in supersonic theory to represent the effects of corners on slender bodies, although a direct physical interpretation is more difficult here.

Since the singular term, $-\frac{1}{2}T(o)\log\left(z-\frac{a^2R^2}{4}\right)$, is a solution to the differential equation and does not affect the boundary conditions either on the body axis or at infinity, it may be subtracted from the integral expressions for the potential to give a solution which is finite in the entire domain.*

---

* This is strictly true only if we exclude stagnation points.

For the region, $z \geq \frac{a^2 r^2}{4}$, influenced by both the elliptic and hyperbolic sources the solution is given by

$$\phi = \frac{1}{2} T(0) \log \left(z - \frac{a^2 r^2}{4} \right) +$$

$$- \frac{1}{4} \int_{z_0}^{0} \left[1 - \frac{z + \xi - \frac{a^2 r^2}{4}}{\sqrt{\left(z - \xi - \frac{a^2 r^2}{4} \right)^2 - a^2 r^2 \xi}} \right] \frac{T(\xi)}{\xi} \, d\xi +$$

$$- \frac{1}{2} \int_{z_0}^{\left(\sqrt{z} - \frac{ar}{2} \right)^2} \left[\frac{z + \xi - \frac{a^2 r^2}{4}}{\sqrt{\left(z - \xi - \frac{a^2 r^2}{4} \right)^2 - a^2 r^2 \xi}} \right] \frac{T(\xi)}{\xi} \, d\xi \quad . \tag{35}$$

For the region, $z \leq \frac{a^2 r^2}{4}$, influenced only by the subsonic sources the solution is given by

$$\phi = \frac{1}{2} T(0) \log \left(\frac{a^2 r^2}{4} - z \right) +$$

$$- \frac{1}{4} \int_{z_0}^{0} \left[1 + \frac{z + \xi - \frac{a^2 r^2}{4}}{\sqrt{\left(z - \xi - \frac{a^2 r^2}{4} \right)^2 - a^2 r^2 \xi}} \right] \frac{T(\xi)}{\xi} \, d\xi \quad .$$

(36)

The disturbance velocity components are obtained by differentiating with respect to z and r, respectively, and then integrating by parts.

For $z \geq \frac{a^2 r^2}{4}$,

$$\phi_z = -\frac{1}{2}\int_{z_0}^{0} \frac{T'(\xi)}{\sqrt{\left(z-\xi-\frac{a^2r^2}{4}\right)^2 - a^2r^2\xi}}\, d\xi + \int_{0}^{\left(\sqrt{z}-\frac{ar}{2}\right)^2} \frac{T'(\xi)}{\sqrt{\left(z-\xi-\frac{a^2r^2}{4}\right)^2 - a^2r^2\xi}}\, d\xi, \tag{37}$$

$$\phi_r = \frac{T(0)}{2r} + \frac{1}{2r}\int_{z_0}^{0} \frac{z-\xi+\frac{a^2r^2}{4}}{\sqrt{\left(z-\xi-\frac{a^2r^2}{4}\right)^2 - a^2r^2\xi}}\, T'(\xi)\, d\xi + \frac{1}{r}\int_{0}^{\left(\sqrt{z}-\frac{ar}{2}\right)^2} \frac{z-\xi+\frac{a^2r^2}{4}}{\sqrt{\left(z-\xi-\frac{a^2r^2}{4}\right)^2 - a^2r^2\xi}}\, T'(\xi)\, d\xi \tag{38}$$

For $z \leq \frac{a^2 r^2}{4}$,

$$\phi_z = -\frac{1}{2}\int_{z_0}^{0} \frac{T'(\xi)}{\sqrt{\left(z-\xi-\frac{a^2r^2}{4}\right)^2 - a^2r^2\xi}}\, d\xi, \tag{39}$$

$$\phi_r = \frac{T(0)}{2r} + \frac{1}{2r}\int_{z_0}^{0} \frac{z-\xi+\frac{a^2r^2}{4}}{\sqrt{\left(z-\xi-\frac{a^2r^2}{4}\right)^2 - a^2r^2\xi}}\, T'(\xi)\, d\xi. \tag{40}$$

The Solution for a Slender Body

If we consider the limit as $r \to 0$ equations 35 through 40 can be greatly simplified. Such a procedure is consistent with the assumptions underlying the derivation of the transonic potential equation and is justified if we are only interested in conditions on the body. The details of this computation are presented in Appendix C. If the origin is transformed back to the nose point, the resulting expressions for the velocity potential and its derivatives are

$$\phi = S(x)\log\frac{ar}{2} + \frac{1}{2}\int_0^x S'(\xi)\log|\xi|\,d\xi + \tag{41}$$
$$-\frac{1}{2}\int_0^x S'(\xi)\log(x-\xi)\,d\xi - \frac{1}{2}\int_{\bar{x}}^x S'(\xi)\log|x-\xi|\,d\xi$$

$$\phi_x = \frac{1}{2}S'(x)\log\frac{a^2r^2}{4x} + \frac{1}{2}\int_0^x \frac{S'(\xi)-S'(x)}{\xi - x}\,d\xi + \frac{1}{2}\int_{\bar{x}}^x \frac{S'(\xi)-S'(x)}{\xi-x}\,d\xi \tag{42}$$

$$\phi_r = \frac{S(x)}{r}. \tag{43}$$

These expressions are valid for $0 \le x \le 1$.

As shown in Appendix C, the expressions for ϕ_x can be expressed in an alternative form.

For $x > \bar{x}$,

$$\phi_x = S'(x)\log\frac{ar\sqrt{x-\bar{x}}}{2} - S'(0)\log\sqrt{x} + \tag{44}$$
$$-\frac{1}{2}\int_0^{\bar{x}} S''(\xi)\log(x-\xi)\,d\xi - \int_{\bar{x}}^x S''(\xi)\log(x-\xi)\,d\xi.$$

For $x < \bar{x}$

$$\phi_x = S'(x)\log\frac{ar\sqrt{\bar{x}-x}}{2} - S'(0)\log\sqrt{x} + \tag{45}$$
$$-\frac{1}{2}\int_0^x S''(\xi)\log(x-\xi)\,d\xi + \frac{1}{2}\int_x^{\bar{x}} S''(\xi)\log(\xi-x)\,d\xi.$$

If equation 45 is compared with the corresponding result for linearized, subsonic, slender body theory* the only difference noted is in the logarithmic term where $\sqrt{1-M_\infty^2}$ has been replaced by $a\sqrt{\bar{x}-x}$. Exactly the same change occurs in the differential equations from which each solution is derived. The point $\bar{x}$ must be interpreted as the tail of the body in comparing with the equivalent linearized result.

A similar result is obtained if equation 44 is compared with the corresponding result for linearized, supersonic, slender body theory.** First, $\sqrt{M_\infty^2-1}$ has been replaced by $a\sqrt{x-\bar{x}}$ in the logarithmic term analogous to the result obtained in the subsonic case. Second, an integral over the subsonic sources appears which is identical to the corresponding term in the linearized subsonic case for the downstream influence of subsonic sources. Here the point $\bar{x}$ must be interpreted as the tail of the subsonic body and the nose of the supersonic body in comparing with the equivalent linearized result.

The Pressure Coefficient and Drag Integral

The pressure coefficient evaluated on the body becomes

$$C_p = -S'(x)\log\frac{a^2\bar{r}^2}{4x} - \left(\frac{d\bar{r}}{dx}\right)^2 + \\ -\int_0^x \frac{S'(\xi)-S'(x)}{\xi-x}\,d\xi - \int_{\bar{x}}^x \frac{S'(\xi)-S'(x)}{\xi-x}\,d\xi \quad (46)$$

The drag is given by

$$\frac{D}{2\pi q_\infty} = \int_0^1 C_p\,S(x)\,dx \quad (6)$$

---

* See Ref. 11, page 189
** See Ref. 11, page 191

The details of this integration are given in Appendix F. The result is

$$\frac{D}{2\pi q_\infty} = -\frac{1}{2} S^2(1) \log \frac{a^2 \bar{r}^2(1)(1-\bar{x})}{4} +$$
$$+ S(1) \int_0^1 S'(x) \log(1-x)\, dx + \frac{1}{2} \int_0^1 \frac{S^2(x)}{x-\bar{x}}\, dx +$$
$$+ \int_0^1 S(x) \left[\int_{\bar{x}}^1 \frac{S'(\xi)}{x-\xi}\, d\xi \right] dx . \qquad (47)$$

If $S(1)=0$ the drag equation further reduces to

$$\frac{D}{2\pi q_\infty} = \int_0^1 S(x) \left[\frac{S(x)}{2(x-\bar{x})} + \int_{\bar{x}}^1 \frac{S'(\xi)}{x-\xi}\, d\xi \right] dx . \qquad (48)$$

It should be noted that in this case the drag is independent of a, suggesting that the drag of a closed body is not strongly dependent on the linearizing assumption. This result is similar to that of linearized supersonic theory where C_D is independent of M_∞.

Example-Symmetrical Parabolic Body

The pressure distribution and drag of a symmetrical parabolic body of revolution can be easily worked out.

For this body

$$S(x) = 4\delta^2 (x - 3x^2 + 2x^3) .$$

Using equation 46

$$\frac{C_p}{\delta^2} = -(12 - 2\sqrt{3}) + (76 - 4\sqrt{3})x - 88x^2 +$$
$$-(4 - 24x + 24x^2) \log \left[-8\sqrt{3}\, \delta^4 \log \delta (\gamma+1) x (1-x)^2 \right]$$
(49)

This is plotted as a solid line in figs. 5, 8, 9, 10, and 11.

Using equation 48 and basing the drag coefficient on the maximum cross-sectional area

$$\frac{C_D}{\delta^2} = \frac{16}{3} + \frac{32}{15}\sqrt{3} \tag{50}$$

or

$$C_D \simeq 9\delta^2.$$

Linearized supersonic theory predicts for the same body

$$C_D = \frac{32}{3}\delta^2.$$

Thus, the predicted transonic drag is 85% of the linearized supersonic drag.

For the parabolic ogive or half-body of revolution the drag integral given here predicts

$$\frac{C_D}{\delta^2} = \frac{1}{3} + \frac{16}{15}\sqrt{3}. \tag{51}$$

Linearized supersonic theory gives

$$\frac{C_D}{\delta^2} = \frac{14}{3}.$$

In both of the latter two cases δ is equal to the maximum thickness divided by twice the length of the half-body. In this case the transonic drag is 47% of the supersonic drag.

From the above results it is evident that in the transonic case a much greater portion of the total drag is carried on the back half of a symmetrical parabolic body of revolution than in the supersonic case. In the transonic case 24% of the drag acts on the front half and 76% on the back half. In the supersonic case 44% is on the front half and 56% on the back half.

Extension to Mach Numbers Near One

This method can be immediately extended to other Mach numbers in the transonic range. If M_∞ is not exactly equal to one the potential equation is given by

$$(1-M_\infty^2)\phi_{xx} + \phi_{rr} + \frac{1}{r}\phi_r = (\gamma+1) M_\infty^2 \phi_x \phi_{xx},$$

or

$$\phi_{rr} + \frac{1}{r}\phi_{rr} = \left[(\gamma+1) M_\infty^2 \phi_x - (1-M_\infty^2)\right] \phi_{xx}. \tag{52}$$

Redefining $\bar{x}$,

$$S'(\bar{x}) = \frac{1-M_\infty^2}{(\gamma+1) M_\infty^2 \log \delta} \tag{53}$$

and a^2,

$$a^2 = (\gamma+1) M_\infty^2 S''(\bar{x}) \log \delta \tag{54}$$

the differential equation reduces to the same form as before (equation 1).

As long as $\bar{x}$ remains on the front portion of the body forward of the maximum thickness point, the solutions previously given, with the appropriate changes in $\bar{x}$ and a^2, should be approximately valid. When $\bar{x}$ occurs at the maximum thickness point this should correspond to the first appearance of supersonic flow. When $\bar{x}$ occurs at the leading edge the subsonic flow regime will have disappeared entirely.

The rate of change of drag coefficient with free stream Mach number at sonic velocity for a closed body of revolution can be easily determined.

$$\frac{\partial C_D}{\partial M_\infty} = \frac{2\pi}{A_{max}} \frac{\partial\left(\frac{D}{2\pi q}\right)}{\partial \bar{x}} \frac{\partial \bar{x}}{\partial M_\infty}$$

where the reference area on which drag coefficient is based is the maximum cross-sectional area.

Differentiating equation 48,

$$\frac{\partial\left(\frac{D}{2\pi q}\right)}{\partial \bar{x}} = \int_0^1 \frac{S(x)\, S'(x)}{x - \bar{x}}\, dx .$$

Differentiating equation 53,

$$S''(\bar{x}) \frac{\partial \bar{x}}{\partial M_\infty} = - \frac{2}{(\gamma+1)\, M_\infty^3 \log \delta} .$$

Evaluating at $M_\infty = 1$,

$$\frac{\partial \bar{x}}{\partial M_\infty} = - \frac{2}{(\gamma+1)\, S''(\bar{x}) \log \delta} .$$

Hence

$$\left(\frac{\partial C_D}{\partial M_\infty}\right)_{M_\infty=1} = - \frac{2}{(\gamma+1)\log\delta}\left[\frac{2\pi}{A_{max}\, S''(\bar{x})} \int_0^1 \frac{S(x)\, S'(x)}{x - \bar{x}}\, dx\right] . \qquad (55)$$

The integral can be approximately evaluated as follows.

$$\int_0^1 \frac{S(x)\,S'(x)}{x-\bar{x}}\,dx = \int_0^{x_{max}} \frac{S(x)\left[S'(x)-S''(\bar{x})(x-\bar{x})\right]}{x-\bar{x}}\,dx + \\ + S''(\bar{x})\int_0^{x_{max}} S(x)\,dx + \int_{x_{max}}^1 \frac{S(x)\,S'(x)}{x-\bar{x}}\,dx .$$

Since

$$\frac{A_{max}}{2\pi} = \int_0^{x_{max}} S(x)\,dx$$

then

$$\left(\frac{\partial C_D}{\partial M_\infty}\right)_{M_\infty=1} = -\frac{2}{(\gamma+1)\log\delta}\left[1 + \frac{2\pi}{A_{max}S''(\bar{x})}\int_0^{x_{max}} \frac{S(x)\left[S'(x)-S''(\bar{x})(x-\bar{x})\right]}{x-\bar{x}}\,dx + \right. \\ \left. + \frac{2\pi}{A_{max}S''(\bar{x})}\int_{x_{max}}^1 \frac{S(x)\,S'(x)}{x-\bar{x}}\,dx\right] . \qquad (56)$$

Within the interval $0 \le x \le x_{max}$, $\dfrac{\left[S'(x)-S''(\bar{x})(x-\bar{x})\right]}{x-\bar{x}}$ is a small quantity which changes sign at $x=\bar{x}$. Furthermore, the magnitude of this quantity is maximum at the endpoints of the interval where $S(x)$ equals zero. Since $S(x)$ is always positive within the interior of the interval, the second term of equation 56 must be small.

Within the interval $x_{max} \le x \le 1$, $S'(x)$ also changes sign. Since $\dfrac{S(x)}{x-\bar{x}}$ is always negative and $S(x)$ equals zero at the endpoints where $S'(x)$ is maximum in magnitude, the third term of equation 56 must also be small.

Thus, the rate of change of drag coefficient with Mach number at sonic velocity is very nearly independent of the shape and is approximately equal to

$$\left(\frac{\partial C_D}{\partial M_\infty}\right)_{M_\infty=1} \simeq -\frac{2}{(\gamma+1)\log_e \delta} . \tag{57}$$

3. COMPARISON WITH EXPERIMENT

McDevitt and Taylor[8] have measured the pressure field and drag of a related series of bodies of revolution of fineness ratio 12 having the maximum thickness at 0.3, 0.4, 0.5, 0.6, and 0.7 of the body length. The data were obtained with the various bodies at zero angle of attack. The Mach number varied from 0.80 to 1.20. The Reynolds number based on body length was 24×10^6. These tests were conducted in the Ames 14-foot, slotted, transonic wind tunnel.

Each body was 72 inches in length and had a maximum diameter of 6 inches. The body shape was determined from the equation

$$r = c\,\frac{\delta}{2}\left[(1-x)-(1-x)^n\right] \qquad x_{max} \leq 0.5$$

$$r = c\,\frac{\delta}{2}\left[\,x - x^n\,\right] \qquad x_{max} \geq 0.5$$

where the constants, c and n, are tabulated below.

Location of maximum cross-sectional area	c	n
0.3	1.712	6.044
0.4	2.364	3.390
0.5	4.000	2.000
0.6	2.364	3.390
0.7	1.712	6.044

The measured pressure coefficients for two Mach numbers, $M_\infty = 1.00$ and $M_\infty = 1.025$, are plotted in each of figs. 3 through 7. The experimental points indicated in these figures are not those

measured but correspond to values at increments in X of 0.05 taken from the recommended fairing through the actual measured data. For this small increment in Mach number, there are quite significant differences in the pressure coefficient. The severe increase in pressure on the aft portion of the body is attributed to the presence of a shock and viscous effects induced by the tunnel walls and the sting support system.

Taylor and Mc Devitt[9] have also measured the pressure field and drag of two additional symmetrical parabolic-arc bodies of revolution of fineness ratio 10 and 14 for similar test conditions as previously described. These data are plotted in figs. 8 and 9.

Drougge[7] has measured the surface pressure and drag of two symmetrical parabolic-arc bodies of revolution of fineness ratio $6\sqrt{2}$ and 6 at sonic speeds. The pressure coefficient data from these tests are presented in figs. 10 and 11.

Page[10], in an unpublished analysis for circular, porous-walled, transonic wind tunnels, has shown that the Mach number error due to wall interference at sonic speeds is given by

$$\Delta M = -0.82 \left(\frac{r^*}{h}\right)^{6/7} \left(\frac{r^*}{x^*}\right)^{2/7},$$

$$M_{WT} = 1 - \Delta M$$

where M_{WT} is the indicated Mach number in the wind tunnel, h is the half-tunnel height, and x^* and r^* are the coordinates of the sonic point on the body surface. For the bodies tested

by Mc Devitt and Taylor this correction varies between $\Delta M = -0.018$ and $\Delta M = -0.027$, hence the data for $M_{WT} = 1.025$ in figs. 3 through 9 very nearly correspond to free flight sonic conditions.

The Mach number correction for the data obtained by Drougge is estimated to be $\Delta M = -0.018$. Thus, the experimental data plotted in figs. 10 and 11 correspond to a free flight Mach number of approximately 0.98.

The theoretical curves plotted in figs. 3 through 11 are based on equation 46 for pressure coefficient. The theoretical calculations for figs. 3, 4, 6, and 7 were carried out on electronic computing equipment. The theoretical curves on figs. 5, 8, 9, 10, and 11 were obtained directly from equation 49 for the pressure distribution on a symmetrical parabolic-arc body of revolution.

The agreement of the theory with the experimental data is fair. The largest discrepancies occur for bodies having the position of maximum thickness forward of the midpoint. As the position of maximum thickness moves aft, the agreement between theory and experiment improves until, for the body with maximum thickness at 0.7 of the body length, the agreement is nearly perfect. This is expected because as the position of maximum thickness moves aft the flow conditions more nearly conform to those assumed in the approximation of nearly uniform acceleration. Also, the effective slenderness is much less for a body with maximum thickness near the rear.

The drag coefficient data, obtained from theory and experiment, for the five symmetrical parabolic-arc bodies of different fineness ratio are presented in figs. 12, 13, 14 and 15. The theoretical point, although determined for a sonic free stream velocity, has been plotted at a

slightly higher Mach number corresponding to the estimated difference between wind tunnel Mach number and the equivalent free flight Mach number. As expected the theoretical drag coefficient compares more favorably with the experimental data than do the pressure coefficients.

Appendix A

Evaluation of the Inversion Integral for the Hyperbolic Sources

From equation 22 of the text

$$\phi = \frac{\pi\sqrt{z'}}{a^2\sqrt{\xi'}}\int_0^\infty \left[Y_1\left(2\frac{\omega}{a}\sqrt{\xi'}\right)J_1\left(2\frac{\omega}{a}\sqrt{z'}\right) - J_1\left(2\frac{\omega}{a}\sqrt{\xi'}\right)Y_1\left(2\frac{\omega}{a}\sqrt{z'}\right)\right] J_0(\omega r)\,\omega\,d\omega. \qquad (22)$$

Writing the integral in terms of Hankel functions

$$\phi = -\frac{\pi\sqrt{z'}}{a^2\sqrt{\xi'}}\,\mathrm{Im}\int_0^\infty H_1^{(1)}\left(2\frac{\omega}{a}\sqrt{z'}\right)H_1^{(2)}\left(2\frac{\omega}{a}\sqrt{\xi'}\right)J_0(\omega r)\,\omega\,d\omega. \qquad (A.1)$$

Interpreting ω as a complex variable and using the illustrated contour the integral can be evaluated along each arc

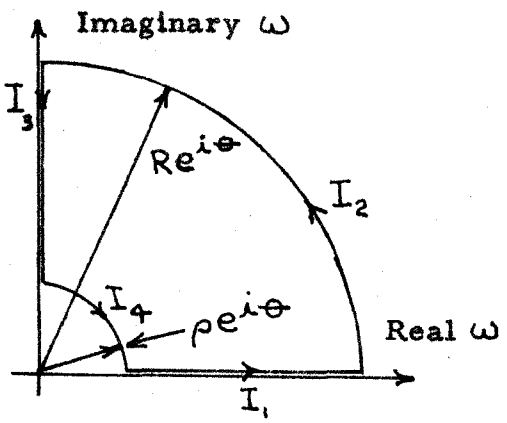

The asymptotic formulas for large values of the argument are given by

$$H_1^{(1)}\left(2\frac{\omega}{a}\sqrt{z'}\right) = \left[\frac{a}{\pi\sqrt{z'}\,Re^{i\theta}}\right]^{1/2} e^{i\left[\frac{2\sqrt{z'}}{a}Re^{i\theta} - \frac{3}{4}\pi\right]} \qquad (A.2)$$

$$-\pi + 2\delta \le \theta \le 2\pi - 2\delta$$

$$H_1^{(2)}\left(2\frac{\omega}{a}\sqrt{\xi'}\right) = \left[\frac{a}{\pi\sqrt{\xi'}\,Re^{i\theta}}\right]^{1/2} e^{-i\left[\frac{2\sqrt{\xi'}}{a}Re^{i\theta} - \frac{3}{4}\pi\right]} \qquad (A.3)$$

$$-2\pi + 2\delta \le \theta \le \pi - 2\delta$$

$$J_0(\omega r) = \left[\frac{1}{2\pi r Re^{i\theta}}\right]^{1/2}\left[e^{i\left[rRe^{i\theta} - \frac{1}{4}\pi\right]} + e^{-i\left[rRe^{i\theta} - \frac{1}{4}\pi\right]}\right]. \qquad (A.4)$$

$$-\pi \le \theta \le \pi$$

where δ is any positive acute angle. Multiplying these quantities

together and transforming the variable of integration to θ , the integrand becomes

$$\frac{ia(Re^{i\theta})^{1/2}}{\pi^{3/2}(2\pi)^{1/2}(z\xi)^{1/4}}\left[e^{-2\frac{R}{a}\sin\theta\left[\sqrt{z}-\sqrt{\xi}+\frac{a\pi}{2}\right]}e^{i\left\{\frac{2R}{a}\cos\theta\left[\sqrt{z}-\sqrt{\xi}+\frac{a\pi}{2}\right]-\frac{\pi}{4}\right\}}+\right.$$

$$\left.+e^{-2\frac{R}{a}\sin\theta\left[\sqrt{z}-\sqrt{\xi}-\frac{a\pi}{2}\right]}e^{i\left\{\frac{2R}{a}\cos\theta\left[\sqrt{z}-\sqrt{\xi}-\frac{a\pi}{2}\right]+\frac{\pi}{4}\right\}}\right].$$

Thus, if $\sqrt{z}-\sqrt{\xi}-\frac{a\pi}{2}>0$, the integral will give no contribution in the limit as $R\to\infty$.

The approximate series for small values of the argument are given by

$$H_1^{(1)}\left(2\frac{\omega}{a}\sqrt{z}\right)=\frac{\sqrt{z}}{a}\rho e^{i\theta}-i\frac{a}{\pi\sqrt{z}\rho e^{i\theta}} \qquad (A.5)$$

$$H_1^{(2)}\left(2\frac{\omega}{a}\sqrt{\xi}\right)=\frac{\sqrt{\xi}}{a}\rho e^{i\theta}+i\frac{a}{\pi\sqrt{\xi}\rho e^{i\theta}} \qquad (A.6)$$

$$J_0(\omega r)=1. \qquad (A.7)$$

The integral becomes

$$I_4=\int_{\frac{\pi}{2}}^{0}\frac{ia^2}{\pi^2\sqrt{z\xi}}d\theta=-i\frac{a^2}{2\pi\sqrt{z\xi}}. \qquad (A.8)$$

The integral along the imaginary axis is obtained by replacing ω by $i\omega$ to give

$$I_3 = \int_0^\infty H_1^{(1)}(2\tfrac{i\omega}{a}\sqrt{z})\,H_1^{(2)}(2\tfrac{i\omega}{a}\sqrt{\xi})\,J_0(i\omega r)\,\omega\,d\omega \qquad \text{(A.9)}$$

Since there are no singularities within the contour, the sum of all contributions must equal zero to give

$$\int_0^\infty H_1^{(1)}(2\tfrac{\omega}{a}\sqrt{z})\,H_1^{(2)}(2\tfrac{\omega}{a}\sqrt{\xi})\,J_0(\omega r)\,\omega\,d\omega =$$

$$= i\frac{a^2}{2\pi\sqrt{z\xi}} - \int_0^\infty H_1^{(1)}(2\tfrac{i\omega}{a}\sqrt{z})\,H_1^{(2)}(2\tfrac{i\omega}{a}\sqrt{\xi})\,J_0(i\omega r)\,\omega\,d\omega \qquad \text{(A.10)}$$

Thus

$$\phi = -\frac{1}{2\xi} + \frac{\pi\sqrt{z}}{a^2\sqrt{\xi}}\,\mathrm{Im}\int_0^\infty H_1^{(1)}(2\tfrac{i\omega}{a}\sqrt{z})\,H_1^{(2)}(2\tfrac{i\omega}{a}\sqrt{\xi})\,J_0(i\omega r)\,\omega\,d\omega \qquad \text{(A.11)}$$

and using the equations

$$H_1^{(1)}(2\tfrac{i\omega}{a}\sqrt{z}) = -\frac{2}{\pi}K_1(2\tfrac{\omega}{a}\sqrt{z}) \qquad \text{(A.12)}$$

$$H_1^{(2)}(2\tfrac{i\omega}{a}\sqrt{\xi}) = \frac{2}{\pi}K_1(2\tfrac{\omega}{a}\sqrt{\xi}) + 2J_1(2\tfrac{i\omega}{a}\sqrt{\xi}) \qquad \text{(A.13)}$$

we obtain

$$\phi = -\frac{1}{2\xi} + i\frac{4\sqrt{z}}{a^2\sqrt{\xi}}\int_0^\infty K_1(2\tfrac{\omega}{a}\sqrt{z})\,J_1(2\tfrac{i\omega}{a}\sqrt{\xi})\,J_0(i\omega r)\,\omega\,d\omega \qquad \text{(A.14)}$$

Integrating by parts

$$\int_0^\infty K_1(2\tfrac{\omega}{a}\sqrt{z})\,J_1(2\tfrac{i\omega}{a}\sqrt{\xi})\,J_0(i\omega r)\,\omega\,d\omega =$$

$$= -\frac{a\omega}{2\sqrt{z}}K_0(2\tfrac{\omega}{a}\sqrt{z})\,J_1(2\tfrac{i\omega}{a}\sqrt{\xi})\,J_0(i\omega r)\Big|_0^\infty +$$

$$+i\frac{a}{2\sqrt{z}}\int_0^\infty K_0(2\tfrac{\omega}{a}\sqrt{z})\left[\frac{2\sqrt{\xi}}{a}J_0(2\tfrac{i\omega}{a}\sqrt{\xi})\,J_0(i\omega r) - r\,J_1(2\tfrac{i\omega}{a}\sqrt{\xi})\,J_1(i\omega r)\right]\omega\,d\omega \qquad \text{(A.15)}$$

If $\sqrt{z}-\sqrt{\xi}-\frac{ar}{2}>0$ the boundary terms give no contribution and we have that

$$\phi = -\frac{1}{2\xi} - \frac{4}{a^2}\int_0^\infty K_0(2\tfrac{\omega}{a}\sqrt{z})\,J_0(2\tfrac{i\omega}{a}\sqrt{\xi})\,J_0(i\omega r)\,\omega\,d\omega +$$

$$+\frac{2r}{a\sqrt{\xi}}\int_0^\infty K_0(2\tfrac{\omega}{a}\sqrt{z})\,J_1(2\tfrac{i\omega}{a}\sqrt{\xi})\,J_1(i\omega r)\,\omega\,d\omega \qquad \text{(A.16)}$$

Watson[12], page 412, and Whittaker and Watson[13], page 326, give formulas for evaluating these integrals. In general we have

$$\int_0^\infty K_\mu(at)\,J_\nu(bt)\,J_\nu(ct)\,t^{\mu+1}\,dt =$$

$$= \frac{1}{2^{\nu+1}}\,\frac{a^\mu}{(bc)^{\mu+1}}\,\frac{\Gamma(\mu+\nu+1)}{\Gamma(\nu+1)}\,\frac{1}{X^{\mu+\nu+1}}\,F\left(\tfrac{1}{2}\mu+\tfrac{1}{2}\nu+1,\tfrac{1}{2}\mu+\tfrac{1}{2}\nu+\tfrac{1}{2};\nu+1;\frac{1}{X^2}\right) \qquad \text{(A.17)}$$

where $X = \frac{a^2+b^2+c^2}{2bc}$.

F denotes the hypergeometric function and for convergence

$$Re(a \pm ib \pm ic) > 0.$$

Using equation A.17 ϕ becomes

$$\phi = -\frac{1}{2\xi} + \frac{1}{ar\sqrt{\xi}X} F(1, \tfrac{1}{2}; 1; \tfrac{1}{X^2}) - \frac{1}{4\xi X^2} F(\tfrac{3}{2}, 1; 2; \tfrac{1}{X^2}) \quad (A.18)$$

where

$$X = -\frac{z - \xi - \frac{a^2r^2}{4}}{ar\sqrt{\xi}}$$

and $\sqrt{z} - \sqrt{\xi} - \frac{ar}{2} > 0$.

The hypergeometric functions can be evaluated in closed form.*

$$F(1, \tfrac{1}{2}; 1; \tfrac{1}{X^2}) = \left(1 - \frac{1}{X^2}\right)^{-1/2} \quad (A.19)$$

$$F(\tfrac{3}{2}, 1; 2; \tfrac{1}{X^2}) = 2X^2\left[\left(1 - \frac{1}{X^2}\right)^{-1/2} - 1\right] \quad (A.20)$$

Substituting for X the potential for a unit strength hyperbolic source is obtained

$$\phi = -\frac{z + \xi - \frac{a^2r^2}{4}}{2\xi\sqrt{\left(z - \xi - \frac{a^2r^2}{4}\right)^2 - a^2r^2\xi}}. \quad (23)$$

---

* See Ref. 14, page 8.

Appendix B

Evaluation of the Inversion Integral for the Elliptic Sources

From equation 28 of the text

$$\phi = \begin{cases} -\frac{2\sqrt{-z}}{a^2\sqrt{-\xi}} \int_0^\infty I_1(2\frac{\omega}{a}\sqrt{-\xi}) K_1(2\frac{\omega}{a}\sqrt{-z}) J_0(\omega r)\, \omega\, d\omega & z<\xi \\ -\frac{2\sqrt{-z}}{a^2\sqrt{-\xi}} \int_0^\infty K_1(2\frac{\omega}{a}\sqrt{-\xi}) I_1(2\frac{\omega}{a}\sqrt{-z}) J_0(\omega r)\, \omega\, d\omega & z>\xi \end{cases} \tag{28}$$

Integrating by parts, for $z < \xi$

$$\phi = \frac{\omega}{a\sqrt{-\xi}} K_0(2\frac{\omega}{a}\sqrt{-z}) I_1(2\frac{\omega}{a}\sqrt{-\xi}) J_0(\omega r) \Big|_0^\infty +$$

$$- \frac{2}{a^2} \int_0^\infty K_0(2\frac{\omega}{a}\sqrt{-z}) I_0(2\frac{\omega}{a}\sqrt{-\xi}) J_0(\omega r)\, \omega\, d\omega +$$

$$+ \frac{r}{a\sqrt{-\xi}} \int_0^\infty K_0(2\frac{\omega}{a}\sqrt{-z}) I_1(2\frac{\omega}{a}\sqrt{-\xi}) J_1(\omega r)\, \omega\, d\omega \tag{B.1a}$$

For $z > \xi$

$$\phi = -\frac{\sqrt{-z}\,\omega}{a\,\xi} K_0(2\frac{\omega}{a}\sqrt{-\xi}) I_1(2\frac{\omega}{a}\sqrt{-z}) J_0(\omega r) \Big|_0^\infty +$$

$$- \frac{2z}{a^2\xi} \int_0^\infty K_0(2\frac{\omega}{a}\sqrt{-\xi}) I_0(2\frac{\omega}{a}\sqrt{-z}) J_0(\omega r)\, \omega\, d\omega +$$

$$- \frac{\sqrt{-z}\, r}{a\,\xi} \int_0^\infty K_0(2\frac{\omega}{a}\sqrt{-\xi}) I_1(2\frac{\omega}{a}\sqrt{-z}) J_1(\omega r)\, \omega\, d\omega \tag{B.1b}$$

The boundary terms are zero at either limit. Using the relations

$$I_0\left(2\frac{\omega}{a}\sqrt{-\xi}\right) = J_0\left(2\frac{i\omega}{a}\sqrt{-\xi}\right) \tag{B.2}$$

$$I_1\left(2\frac{\omega}{a}\sqrt{-\xi}\right) = -i\,J_1\left(2\frac{i\omega}{a}\sqrt{-\xi}\right) \tag{B.3}$$

the integrals can be put in the proper form corresponding to the integration formula, equation A. 17.

For $z < \xi$

$$\phi = -\frac{2}{a^2}\int_0^\infty K_0\left(2\frac{\omega}{a}\sqrt{-z}\right) J_0\left(2\frac{i\omega}{a}\sqrt{-\xi}\right) J_0(\omega r)\,\omega\,d\omega +$$

$$+\frac{r}{a\sqrt{-\xi}}\int_0^\infty K_0\left(2\frac{\omega}{a}\sqrt{-z}\right) J_1\left(2\frac{i\omega}{a}\sqrt{-\xi}\right) J_1(\omega r)\,\omega\,d\omega \tag{B.4a}$$

For $z > \xi$

$$\phi = -\frac{2z}{a^2\xi}\int_0^\infty K_0\left(2\frac{\omega}{a}\sqrt{-\xi}\right) J_0\left(2\frac{i\omega}{a}\sqrt{-z}\right) J_0(\omega r)\,\omega\,d\omega +$$

$$+i\frac{r\sqrt{-z}}{a\xi}\int_0^\infty K_0\left(2\frac{\omega}{a}\sqrt{-\xi}\right) J_1\left(2\frac{i\omega}{a}\sqrt{-z}\right) J_1(\omega r)\,\omega\,d\omega \tag{B.4b}$$

After carrying out the integrations we obtain, for either case

$$\phi = -\frac{1}{4\xi} - \frac{z+\xi-\frac{a^2r^2}{4}}{4\xi\sqrt{\left(z-\xi-\frac{a^2r^2}{4}\right)^2 - a^2r^2\xi}}. \tag{30}$$

Although equation 30 has been worked out for $z<0$, it is valid in the extended domain $z < \frac{a^2r^2}{4}$.

Appendix C

The Velocity Potential in the Slender Body Limit

Equations 35 through 40 for the velocity potential and the velocity components can be simplified by taking the limit as $\kappa \to 0$ retaining only the dominant terms.

For $z \geq \frac{a^2 r^2}{4}$,

$$\phi = \frac{1}{2} T(0) \log\left(z - \frac{a^2 r^2}{4}\right) +$$

$$-\frac{1}{4}\int_{z_0}^{0}\left[1 - \frac{z+\xi-\frac{a^2r^2}{4}}{\sqrt{\left(z-\xi-\frac{a^2r^2}{4}\right)^2 - a^2r^2\xi}}\right]\frac{T(\xi)}{\xi}\,d\xi +$$

$$-\frac{1}{2}\int_{z_0}^{\left(\sqrt{z}-\frac{ar}{2}\right)^2}\left[\frac{z+\xi-\frac{a^2r^2}{4}}{\sqrt{\left(z-\xi-\frac{a^2r^2}{4}\right)^2 - a^2r^2\xi}}\right]\frac{T(\xi)}{\xi}\,d\xi \qquad (35)$$

The integrand in the third term will be singular at the upper limit. To investigate this singularity we introduce a new integration variable, θ, where

$$\xi = \left(\sqrt{z} - \frac{ar}{2}\cosh\theta\right)^2 \qquad (C.1)$$

The potential becomes

$$\phi = \frac{1}{2}T(0)\log\left(z - \frac{a^2r^2}{4}\right) +$$

$$-\frac{1}{4}\int_{z_0}^{0}\left[1 - \frac{z+\xi-\frac{a^2r^2}{4}}{\sqrt{\left(z-\xi-\frac{a^2r^2}{4}\right)^2 - a^2r^2\xi}}\right]\frac{T(\xi)}{\xi}\,d\xi +$$

$$-\frac{1}{2}\int_{z_0}^{\left(\sqrt{z}-\frac{ar}{2}\right)^2-\varepsilon}\left[\frac{z+\xi-\frac{a^2r^2}{4}}{\sqrt{\left(z-\xi-\frac{a^2r^2}{4}\right)^2 - a^2r^2\xi}}\right]\frac{T(\xi)}{\xi}\,d\xi +$$

$$-\int_{0}^{\cosh^{-1}\frac{2}{ar}\left[\sqrt{z}-\sqrt{\left(\sqrt{z}-\frac{ar}{2}\right)^2-\varepsilon}\right]}\frac{\left[1-\frac{ar}{2\sqrt{z}}\cosh\theta+\frac{a^2r^2}{8z}\sinh^2\theta\right]}{\sqrt{1-\frac{ar}{2\sqrt{z}}\cosh\theta+\frac{a^2r^2}{16z}\sinh^2\theta}}\frac{T\left[\left(\sqrt{z}-\frac{ar}{2}\cosh\theta\right)^2\right]}{\left[1-\frac{ar}{2\sqrt{z}}\cosh\theta\right]}\,d\theta \qquad \text{(C.2)}$$

Taking the limit as $r \longrightarrow 0$, $(\varepsilon/r \longrightarrow \infty)$

$$\phi = \frac{1}{2}T(0)\log z + \frac{1}{2}\int_{z_0}^{0}\frac{T(\xi)}{z-\xi}\,d\xi +$$

$$-\frac{1}{2}\int_{z_0}^{z-\varepsilon}\frac{z+\xi}{z-\xi}\,\frac{T(\xi)}{\xi}\,d\xi - T(z)\int_{0}^{\cosh^{-1}\frac{\varepsilon}{ar\sqrt{z}}}d\theta \qquad \text{(C.3)}$$

Integrating the second and third terms by parts

$$\int_{z_o}^{0} \frac{T(\xi)}{z-\xi}\, d\xi = -T(0)\log z + \int_{z_o}^{0} T'(\xi)\log(z-\xi)\, d\xi \qquad \text{(C.4)}$$

$$\int_{z_o}^{z-\varepsilon} \frac{z+\xi}{z-\xi}\,\frac{T(\xi)}{\xi}\, d\xi = T(z-\varepsilon)\log(z-\varepsilon) - 2T(z-\varepsilon)\log\varepsilon +$$

$$-\int_{z_o}^{z-\varepsilon} T'(\xi)\log|\xi|\, d\xi + 2\int_{z_o}^{z-\varepsilon} T'(\xi)\log(z-\xi)\, d\xi \qquad \text{(C.5)}$$

For the fourth term

$$\lim_{r\to 0}\int_{0}^{\cosh^{-1}\frac{\varepsilon}{ar\sqrt{z'}}} d\theta = \log\frac{2\varepsilon}{ar\sqrt{z'}} \qquad \text{(C.6)}$$

Combining terms and taking the limit as $\varepsilon \to 0$

$$\phi = T(z)\log\frac{ar}{2} + \frac{1}{2}\int_{z_o}^{z} T'(\xi)\log|\xi|\, d\xi +$$

$$-\frac{1}{2}\int_{z_o}^{0} T'(\xi)\log(z-\xi)\, d\xi - \int_{0}^{z} T'(\xi)\log(z-\xi)\, d\xi \qquad \text{(C.7)}$$

Integrating each integral by parts and then differentiating with respect to z

$$\phi_z = T'(z)\log\frac{ar+\sqrt{z}}{2} - T'(z_0)\log\sqrt{z-z_0} +$$

$$-\frac{1}{2}\int_{z_0}^{0} T''(\xi)\log(z-\xi)\,d\xi - \int_{0}^{z} T''(\xi)\log(z-\xi)\,d\xi \qquad (C.8)$$

Equation 44 of the text is obtained by transforming the independent variable from z to X.

Differentiating equation C.7 with respect to r

$$\phi_r = \frac{T(z)}{r}. \qquad (C.9)$$

Thus,

$$\lim_{r\to 0}(r\phi_r) = T(z)$$

which verifies the boundary condition of tangent flow on the body in the hyperbolic regime.

For $z \le \frac{a^2r^2}{4}$,

$$\phi = \frac{1}{2}T(0)\log\left(\frac{a^2r^2}{4} - z\right) +$$

$$-\frac{1}{4}\int_{z_0}^{0}\left[1 + \frac{z+\xi-\frac{a^2r^2}{4}}{\sqrt{\left(z-\xi-\frac{a^2r^2}{4}\right)^2 - a^2r^2\xi}}\right]\frac{T(\xi)}{\xi}\,d\xi \qquad (36)$$

To investigate the singularity of the integrand let

$$\xi = -\left(\sqrt{-z} - \frac{ar}{2}\tan\theta\right)^2 \tag{C.10}$$

The potential becomes

$$\phi = \frac{1}{2}T(0)\log\left(\frac{a^2r^2}{4} - z\right) +$$

$$-\frac{1}{4}\int_{z_0}^{z-\varepsilon}\left[1 + \frac{z+\xi-\frac{a^2r^2}{4}}{\sqrt{\left(z-\xi-\frac{a^2r^2}{4}\right)^2 - a^2r^2\xi}}\right]\frac{T(\xi)}{\xi}\,d\xi +$$

$$-\frac{1}{2}\int_{\tan^{-1}\frac{2}{ar}\left[\sqrt{-z}-\sqrt{-z-\varepsilon}\right]}^{\tan^{-1}\frac{2}{ar}\left[\sqrt{-z}-\sqrt{-z+\varepsilon}\right]}\frac{\left[1 - \frac{ar}{2\sqrt{-z}}\tan\theta - \frac{a^2r^2}{8z}\sec^2\theta\right]}{\sqrt{1 - \frac{ar}{2\sqrt{-z}}\tan\theta - \frac{a^2r^2}{16z}\sec^2\theta}}\frac{T\left[-\left(\sqrt{-z} - \frac{ar}{2}\tan\theta\right)^2\right]}{\left[1 - \frac{ar}{2\sqrt{-z}}\tan\theta\right]}\frac{d\theta}{\cos\theta} +$$

$$-\frac{1}{4}\int_{z+\varepsilon}^{0}\left[1 + \frac{z+\xi-\frac{a^2r^2}{4}}{\sqrt{\left(z-\xi-\frac{a^2r^2}{4}\right)^2 - a^2r^2\xi}}\right]\frac{T(\xi)}{\xi}\,d\xi \tag{C.11}$$

Taking the limit as $r \to 0$

$$\phi = \frac{1}{2}T(0)\log(-z) - \frac{1}{2}\int_{z_0}^{z-\varepsilon}\frac{z}{z-\xi}\,\frac{T(\xi)}{\xi}\,d\xi +$$

$$-\frac{1}{2}T(z)\int_{\tan^{-1}\frac{-\varepsilon}{ar\sqrt{-z}}}^{\tan^{-1}\frac{\varepsilon}{ar\sqrt{-z}}}\frac{d\theta}{\cos\theta} + \frac{1}{2}\int_{z+\varepsilon}^{0}\frac{T(\xi)}{z-\xi}\,d\xi \tag{C.12}$$

Integrating the second and fourth terms by parts

$$\int_{z_0}^{z-\varepsilon} \frac{z}{\xi(z-\xi)} T(\xi)\, d\xi = T(z-\varepsilon)\log(-z+\varepsilon) - T(z-\varepsilon)\log\varepsilon +$$

$$-\int_{z_0}^{z-\varepsilon} T'(\xi)\log(-\xi)\, d\xi + \int_{z_0}^{z-\varepsilon} T'(\xi)\log(z-\xi)\, d\xi \qquad \text{(C.13)}$$

$$\int_{z+\varepsilon}^{0} \frac{T(\xi)}{z-\xi}\, d\xi = T(z+\varepsilon)\log\varepsilon - T(0)\log(-z) +$$

$$+\int_{z+\varepsilon}^{0} T'(\xi)\log(\xi - z)\, d\xi \qquad \text{(C.14)}$$

For the third term

$$\lim_{r\to 0} \int_{\tan^{-1}\frac{-\varepsilon}{ar\sqrt{-z}}}^{\tan^{-1}\frac{\varepsilon}{ar\sqrt{-z}}} \frac{d\theta}{\cos\theta} = 2\log\frac{2\varepsilon}{ar\sqrt{-z}} \qquad \text{(C.15)}$$

Combining terms and taking the limit as $\varepsilon \to 0$

$$\phi = T(z)\log\frac{ar}{2} + \frac{1}{2}\int_{z_0}^{z} T'(\xi)\log(-\xi)\, d\xi +$$

$$-\frac{1}{2}\int_{z_0}^{z} T'(\xi)\log(z-\xi)\, d\xi + \frac{1}{2}\int_{z}^{0} T'(\xi)\log(\xi - z)\, d\xi \qquad \text{(C.16)}$$

If the limits of integration are changed in equations C. 7 and C. 16 they both take the form

$$\phi = T(z)\log\frac{ar}{2} + \frac{1}{2}\int_{z_0}^{z} T'(\xi)\log|\xi|\, d\xi +$$

$$-\frac{1}{2}\int_{z_0}^{z} T'(\xi)\log(z-\xi)\, d\xi - \frac{1}{2}\int_{0}^{z} T'(\xi)\log|z-\xi|\, d\xi \qquad \text{(C.17)}$$

Equation 41 of the text is obtained by transforming the independent variable from z to X .

Integrating the second, third, and fourth terms of equation C. 16 by parts and then differentiating with respect to z

$$\phi_z = T'(z)\log\frac{ar\sqrt{-z}}{2} - T'(z_0)\log\sqrt{z-z_0} + \\ -\frac{1}{2}\int_{z_0}^{z} T''(\xi)\log(z-\xi)\,d\xi + \frac{1}{2}\int_{z}^{0} T''(\xi)\log(\xi-z)\,d\xi \quad \text{(C.18)}$$

Equation 45 of the text is obtained by transforming the independent variable from z to X .

If the four integrals appearing in equations C. 8 and C. 18 for ϕ_z are integrated by parts, the resultant expressions reduce to the same algebraic form.

Integrating by parts

$$\int_{z_0}^{0} T''(\xi)\log(z-\xi)\,d\xi = \left[T'(z)-T'(z_0)\right]\log(z-z_0) + \\ -T'(z)\log z - \int_{z_0}^{0}\frac{T'(\xi)-T'(z)}{\xi-z}\,d\xi \quad \text{(C.19)}$$

$$\int_{0}^{z} T''(\xi)\log(z-\xi)\,d\xi = T'(z)\log z + \\ -\int_{0}^{z}\frac{T'(\xi)-T'(z)}{\xi-z}\,d\xi \quad \text{(C.20)}$$

$$\int_{z_0}^{z} T''(\xi)\log(z-\xi)\,d\xi = \left[T'(z)-T'(z_0)\right]\log(z-z_0) + \\ -\int_{z_0}^{z}\frac{T'(\xi)-T'(z)}{\xi-z}\,d\xi \quad \text{(C.21)}$$

$$\int_z^0 T''(\xi)\log(\xi - z)\,d\xi = -T'(z)\log(-z) + \\ -\int_z^0 \frac{T'(\xi) - T'(z)}{\xi - z}\,d\xi \,. \qquad (C.22)$$

Combining these integrals

$$\phi_z = \frac{1}{2}T'(z)\log\frac{a^2 r^2}{4(z - z_0)} + \frac{1}{2}\int_{z_0}^{z}\frac{T'(\xi) - T'(z)}{\xi - z}\,d\xi + \\ + \frac{1}{2}\int_0^{z}\frac{T'(\xi) - T'(z)}{\xi - z}\,d\xi \qquad z_0 \le z \le z_1 \,. \qquad (C.23)$$

Equation 42 of the text is obtained by transforming the independent variable from z to X.

Differentiating equation C.16 with respect to r

$$\phi_r = \frac{T(z)}{r} \,. \qquad (C.24)$$

Thus

$$\lim_{r \to 0}(r\phi_r) = T(z)$$

which verifies the boundary condition of tangent flow on the body in the elliptic regime.

Appendix D

Singular Behavior of the Integrated Solution

The potential obtained by integrating over the source distribution is given by

$$z > \frac{a^2\pi^2}{4}$$

$$\phi = -\frac{1}{4}\int_{z_0}^{0}\left[1 - \frac{z+\xi-\frac{a^2\pi^2}{4}}{\sqrt{\left(z-\xi-\frac{a^2\pi^2}{4}\right)^2 - a^2\pi^2\xi}}\right]\frac{T(\xi)}{\xi}\,d\xi +$$

$$-\frac{1}{2}\int_{z_0}^{\left(\sqrt{z}-\frac{a\pi}{2}\right)^2}\left[\frac{z+\xi-\frac{a^2\pi^2}{4}}{\sqrt{\left(z-\xi-\frac{a^2\pi^2}{4}\right)^2 - a^2\pi^2\xi}}\right]\frac{T(\xi)}{\xi}\,d\xi \qquad (31)$$

$$z < \frac{a^2\pi^2}{4}$$

$$\phi = -\frac{1}{4}\int_{z_0}^{0}\left[1 + \frac{z+\xi-\frac{a^2\pi^2}{4}}{\sqrt{\left(z-\xi-\frac{a^2\pi^2}{4}\right)^2 - a^2\pi^2\xi}}\right]\frac{T(\xi)}{\xi}\,d\xi \qquad (32)$$

Integrating by parts

$$z > \frac{a^2\pi^2}{4}$$

$$\phi = -\frac{1}{2}T(0)\log\left(z-\frac{a^2\pi^2}{4}\right) + \frac{1}{2}T(0)\log\frac{a\pi}{2} + \frac{1}{2}\int_{z_0}^{\left(\sqrt{z}-\frac{a\pi}{2}\right)^2}T'(\xi)\log(-\xi)\,d\xi +$$

$$-\frac{1}{4}\int_{z_0}^{0}T'(\xi)\log\left|\frac{\left(z-\frac{a^2\pi^2}{4}\right)X^{1/2} + \left(z-\frac{a^2\pi^2}{4}\right)^2 - \xi\left(z+\frac{a^2\pi^2}{4}\right)}{X^{1/2}+\xi-\left(z+\frac{a^2\pi^2}{4}\right)}\right|d\xi +$$

$$-\frac{1}{2}\int_{0}^{\left(\sqrt{z}-\frac{a\pi}{2}\right)^2}T'(\xi)\log\left|\frac{\left(z-\frac{a^2\pi^2}{4}\right)X^{1/2} + \left(z-\frac{a^2\pi^2}{4}\right)^2 - \xi\left(z+\frac{a^2\pi^2}{4}\right)}{X^{1/2}+\xi-\left(z+\frac{a^2\pi^2}{4}\right)}\right|d\xi \qquad (D.1a)$$

$z < \frac{a^2 r^2}{4}$

$$\phi = -\frac{1}{2} T(0) \log\left(\frac{a^2 r^2}{4} - z\right) + \frac{1}{2} T(0) \log \frac{ar}{2} +$$

$$-\frac{1}{4} \int_{z_0}^{0} T'(\xi) \log \left| \frac{\left(z - \frac{a^2 r^2}{4}\right) X^{1/2} + \left(z - \frac{a^2 r^2}{4}\right)^2 - \xi\left(z + \frac{a^2 r^2}{4}\right)}{X^{1/2} + \xi - \left(z + \frac{a^2 r^2}{4}\right)} \right| d\xi +$$

$$+\frac{1}{2} \int_{z_0}^{0} T'(\xi) \log(-\xi)\, d\xi \qquad \text{(D. 1b)}$$

where

$$X = \left(z - \xi - \frac{a^2 r^2}{4}\right)^2 - a^2 r^2 \xi$$

The integrals are all finite as $z \to \frac{a^2 r^2}{4}$ hence the singularity is given by the boundary term,

$$\phi_{sing} = -\frac{1}{2} T(0) \log\left| z - \frac{a^2 r^2}{4} \right| \qquad (33)$$

Appendix E

Similarity Solutions for a Source Located at the Origin

The solution for the potential due to a source located at the origin can be easily obtained by a similarity transformation.

First, we consider a discrete source of unit strength at the origin.

$$\phi_{rr} + \frac{1}{r}\phi_r - a^2 z \phi_{zz} = \frac{\delta(r)\,\delta(z)}{r} \tag{E.1}$$

A similarity analysis shows that the solution must be of the form

$$\phi = \frac{1}{z} f\left(\frac{a^2 r^2}{z}\right). \tag{E.2}$$

Letting $\eta = \frac{a^2 r^2}{4z}$ the differential equation becomes

$$\eta(1-\eta) f_{\eta\eta} + (1-4\eta) f_\eta - 2f = 0. \tag{E.3}$$

The solution for ϕ is

$$\phi = \frac{1}{z} F\left(1, 2; 1; \frac{a^2 r^2}{4z}\right) = \frac{z}{\left(z - \frac{a^2 r^2}{4}\right)^2}. \tag{E.4}$$

This checks the behavior of a source at the origin obtained in equation 34.

As a second example, we consider a line of sources having a discontinuous jump in strength at the origin.

$$\phi_{rr} + \frac{1}{r}\phi_r - a^2 z \phi_{zz} = \frac{\delta(r)\,H(z)}{r} \tag{E.5}$$

where $H(z)$ is the Heaviside function. The solution must be of the form

$$\phi = f\left(\frac{a^2 r^2}{z}\right). \tag{E.6}$$

Letting $\eta = \frac{a^2 r^2}{4z}$ the differential equation becomes

$$\eta(1-\eta) f_{\eta\eta} + (1-2\eta) f_\eta = 0. \qquad \text{(E. 7)}$$

The solution is

$$\phi = C_0 + C_1 \log \frac{4\left(z - \frac{a^2 r^2}{4}\right)}{a^2 r^2}. \qquad \text{(E. 8)}$$

The logarithmic divergence of the potential on the line $z = \frac{a^2 r^2}{4}$ is identical to the behavior of the incomplete potential determined in equations D. 1

Appendix F

The Drag Integral

The drag is given by

$$\frac{D}{2\pi q_\infty} = \int_0^1 C_p S(x)\, dx. \tag{6}$$

Substituting equation 46 for the pressure coefficient into equation 6 we obtain

$$-\frac{D}{2\pi q_\infty} = I_1 + I_2 + I_3 + I_4$$

where

$$I_1 = \int_0^1 S(x)\, S'(x) \log \frac{a^2 \bar{r}^2}{4x}\, dx \tag{F. 1a}$$

$$I_2 = \int_0^1 S(x) \left(\frac{d\bar{r}}{dx}\right)^2 dx \tag{F. 1b}$$

$$I_3 = \int_0^1 S(x) \left[\int_0^x \frac{S'(\xi) - S'(x)}{\xi - x}\, d\xi \right] dx \tag{F. 1c}$$

$$I_4 = \int_0^1 S(x) \left[\int_{\bar{x}}^x \frac{S'(\xi) - S'(x)}{\xi - x}\, d\xi \right] dx. \tag{F. 1d}$$

Integrating I_1 by parts

$$I_1 = \frac{1}{2} S^2(1) \log \frac{a^2 \bar{r}^2(1)}{4} - \int_0^1 S(x) \left(\frac{d\bar{r}}{dx}\right)^2 dx +$$

$$- \int_0^1 S(x)\, S'(x) \log x\, dx. \tag{F. 2}$$

Using the relation

$$\int_0^x \frac{S'(\xi)-S'(x)}{\xi - x}\,d\xi = S'(x)\log x - \frac{d}{dx}\int_0^x S'(\xi)\log(x-\xi)\,d\xi \qquad \text{(F.3)}$$

and integrating by parts, I_3 becomes

$$I_3 = -S(1)\int_0^1 S'(x)\log(1-x)\,dx + \int_0^1 S(x)S'(x)\log x\,dx +$$

$$+\int_0^1 S'(x)\left[\int_0^x S'(\xi)\log(x-\xi)\,d\xi\right]dx. \qquad \text{(F.4)}$$

The last integral in equation F.4 is put in a more convenient form by interchanging the role of X and ξ, interchanging the order of integration, and then splitting up into three separate integrals as follows-

$$\int_0^1 S'(x)\left[\int_0^x S'(\xi)\log(x-\xi)\,d\xi\right]dx = \int_0^1 S'(\xi)\left[\int_0^\xi S'(x)\log(\xi-x)\,dx\right]d\xi =$$

$$= \int_0^1 S'(x)\left[\int_x^1 S'(\xi)\log(\xi-x)\,d\xi\right]dx =$$

$$= \int_0^{\bar{x}} S'(x)\left[\int_x^{\bar{x}} S'(\xi)\log(\xi-x)\,d\xi\right]dx +$$

$$+\int_0^{\bar{x}} S'(x)\left[\int_{\bar{x}}^1 S'(\xi)\log(\xi-x)\,d\xi\right]dx +$$

$$+\int_{\bar{x}}^1 S'(x)\left[\int_x^1 S'(\xi)\log(\xi-x)\,d\xi\right]dx. \qquad \text{(F.5)}$$

Using the relation

$$\int_{\bar{x}}^{x} \frac{S'(\xi)-S'(x)}{\xi - x}\, d\xi = S'(x)\log|x-\bar{x}| - \frac{d}{dx}\int_{\bar{x}}^{x} S'(\xi)\log|\xi-x|\, d\xi \qquad \text{(F.6)}$$

and integrating by parts, I_4 **becomes**

$$I_4 = -S(1)\int_{\bar{x}}^{1} S'(x)\log(1-x)\,dx +$$

$$+\int_{0}^{1} S(x)\,S'(x)\log|x-\bar{x}|\,dx +$$

$$+\int_{0}^{1} S'(x)\left[\int_{\bar{x}}^{x} S'(\xi)\log|\xi-x|\,d\xi\right]dx \qquad \text{(F.7)}$$

Splitting the last integral of equation F. 7 into two parts

$$\int_{0}^{1} S'(x)\left[\int_{\bar{x}}^{x} S'(\xi)\log|\xi-x|\,d\xi\right]dx =$$

$$= \int_{0}^{\bar{x}} S'(x)\left[\int_{\bar{x}}^{x} S'(\xi)\log(\xi-x)\,d\xi\right]dx +$$

$$+\int_{\bar{x}}^{1} S'(x)\left[\int_{\bar{x}}^{x} S'(\xi)\log(x-\xi)\,d\xi\right]dx \qquad \text{(F.8)}$$

Combining equations F. 1b, F.2, F.4, F.5, F. 7, and F.8 the drag becomes

$$\frac{D}{2\pi q_\infty} = -\frac{1}{2}S^2(1)\log\frac{a^2\bar{r}^2(1)}{4} + S(1)\int_0^1 S'(x)\log(1-x)\,dx +$$

$$+S(1)\int_{\bar{x}}^1 S'(x)\log(1-x)\,dx - \int_0^1 S(x)\,S'(x)\log|x-\bar{x}|\,dx +$$

$$-\int_0^1 S'(x)\left[\int_{\bar{x}}^1 S'(\xi)\log|\xi-x|\,d\xi\right]dx. \qquad \text{(F. 9)}$$

Integrating the fourth and fifth terms of equation F. 9 by parts the drag equation reduces to

$$\frac{D}{2\pi q_\infty} = -\frac{1}{2}S^2(1)\log\frac{a^2\bar{r}^2(1)(1-\bar{x})}{4} +$$

$$+S(1)\int_0^1 S'(x)\log(1-x)\,dx + \frac{1}{2}\int_0^1 \frac{S^2(x)}{x-\bar{x}}\,dx +$$

$$+\int_0^1 S(x)\left[\int_{\bar{x}}^1 \frac{S'(\xi)}{x-\xi}\,d\xi\right]dx. \qquad (47)$$

If $S(1)=0$ then the drag equation further reduces to

$$\frac{D}{2\pi q_\infty} = \int_0^1 S(x)\left[\frac{S(x)}{2(x-\bar{x})} + \int_{\bar{x}}^1 \frac{S'(\xi)}{x-\xi}\,d\xi\right]dx. \qquad (48)$$

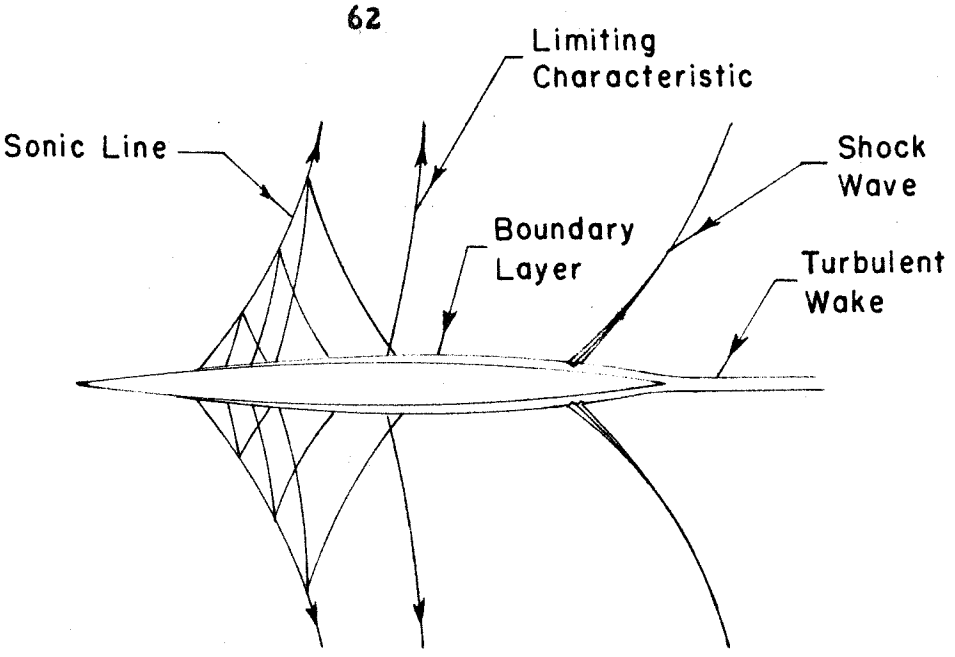

FIG. 1 TRANSONIC FLOW ABOUT A BODY OF REVOLUTION

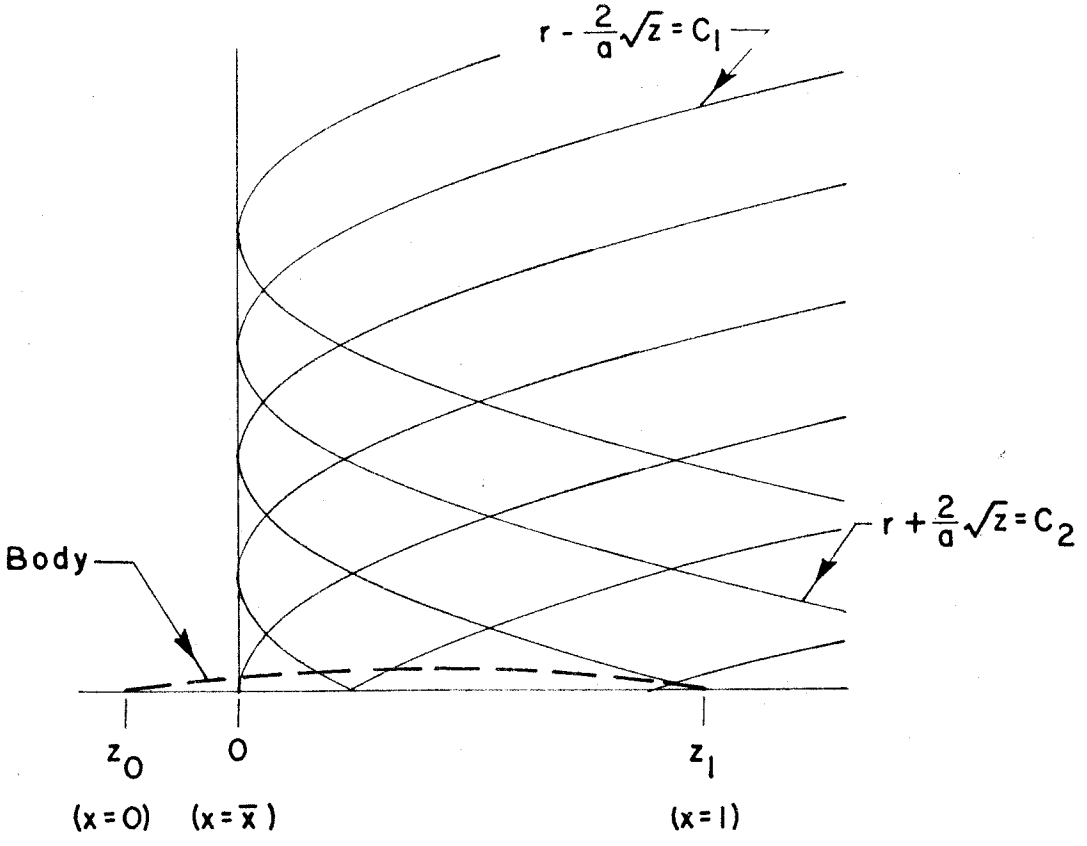

FIG. 2 CHARACTERISTICS FOR $\phi_{rr} + \frac{1}{r}\phi_r = a^2 z \phi_{zz}$

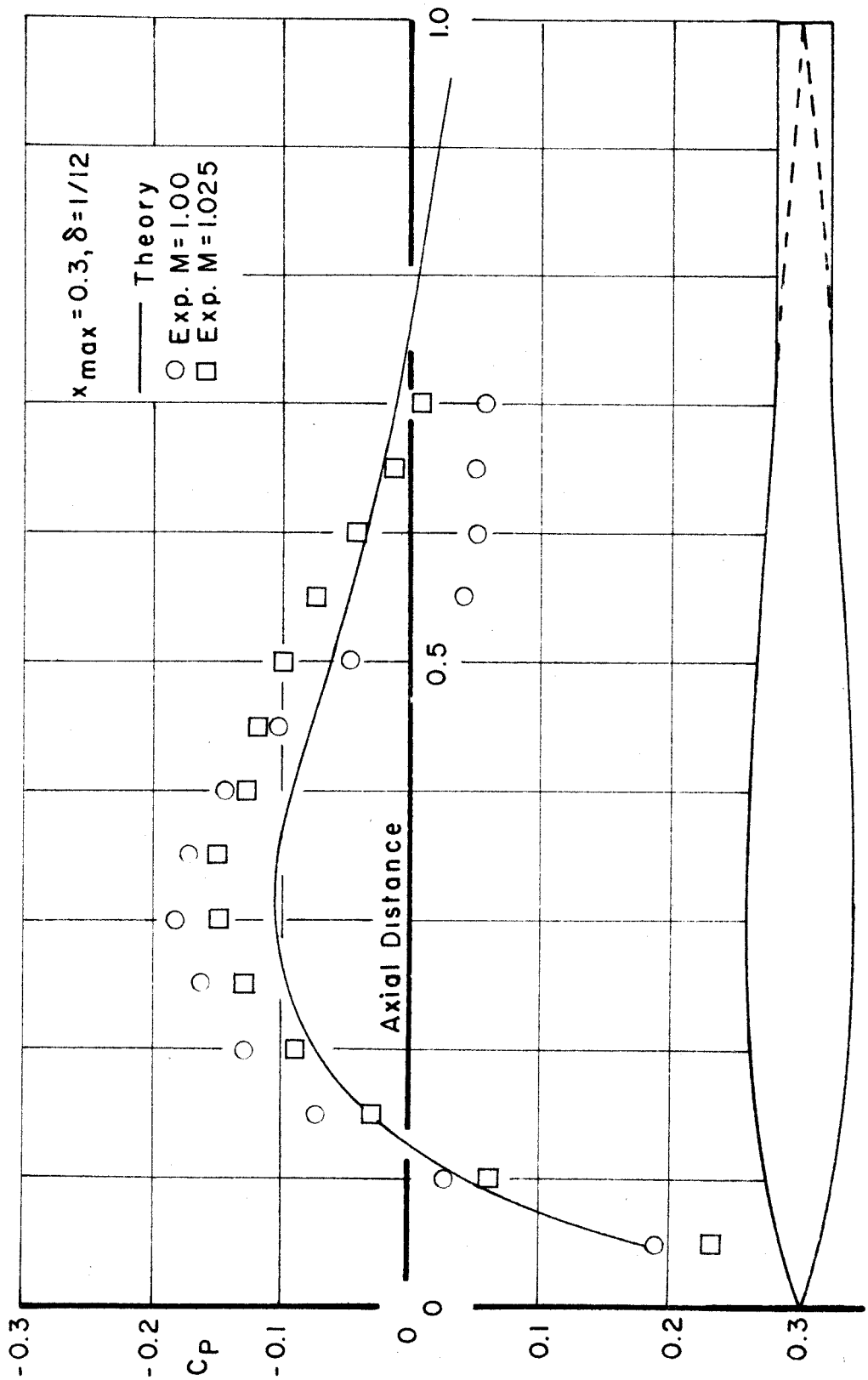

FIG.3 SLENDER BODY PRESSURE DISTRIBUTION

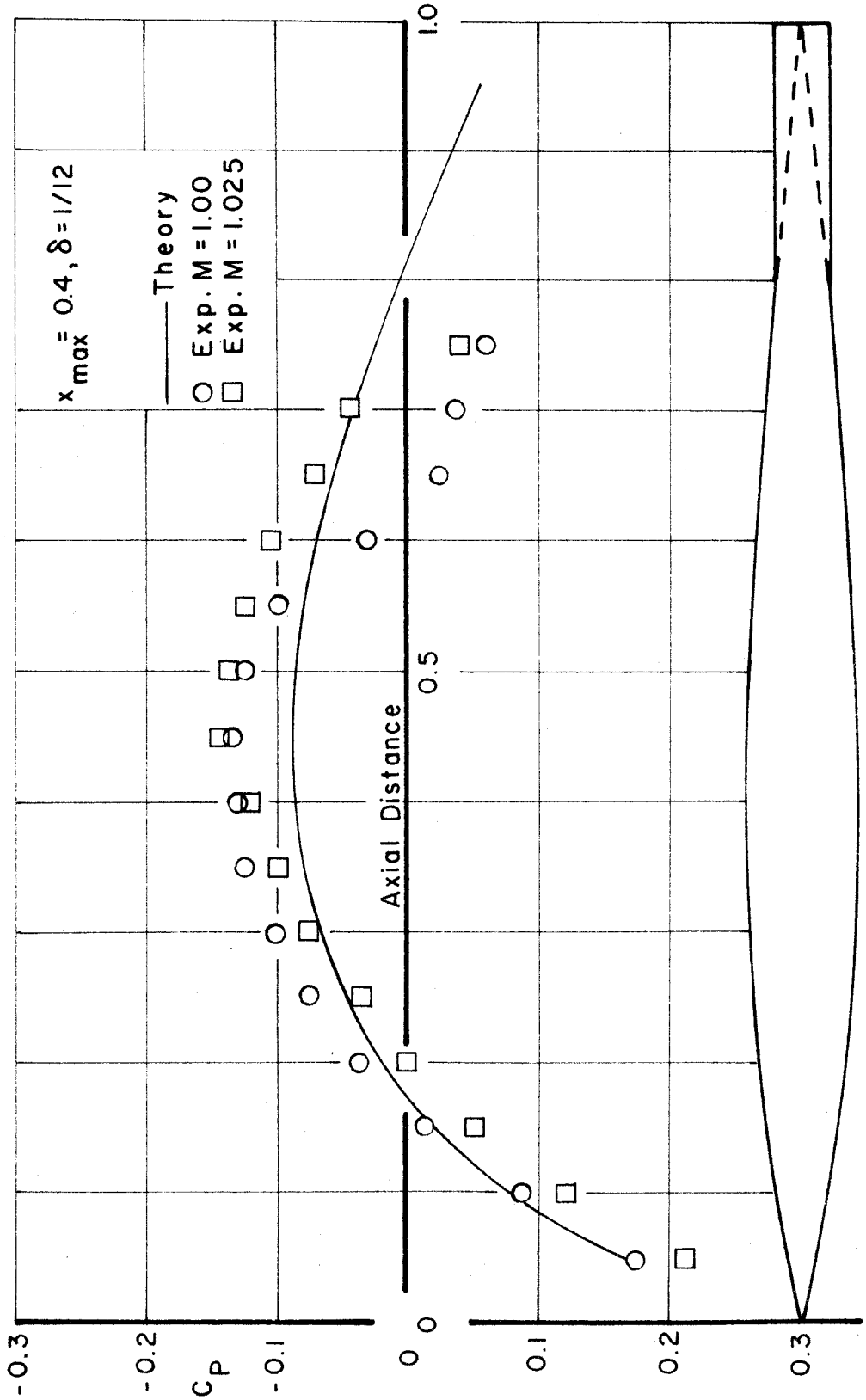

FIG. 4 SLENDER BODY PRESSURE DISTRIBUTION

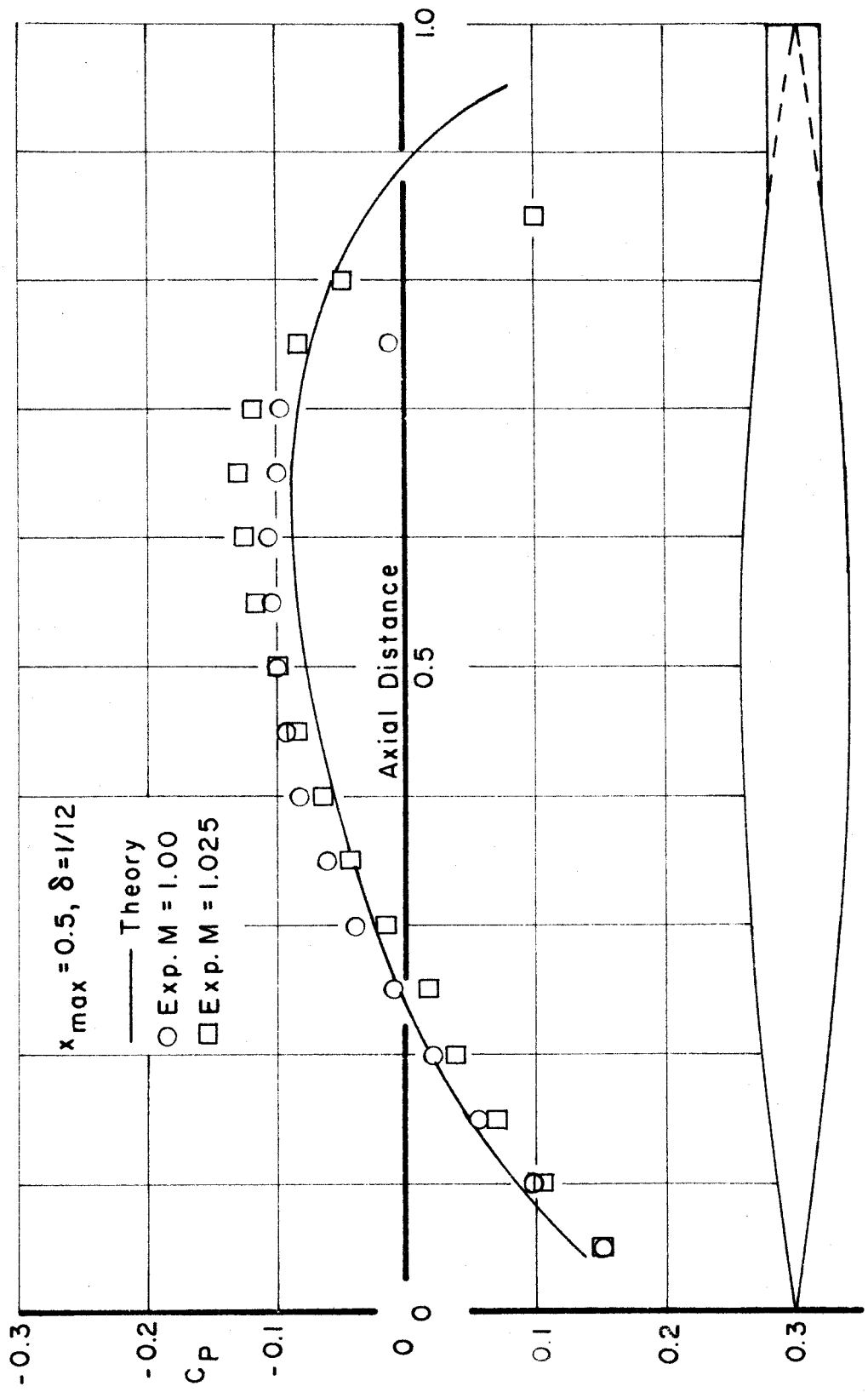

FIG. 5 SLENDER BODY PRESSURE DISTRIBUTION

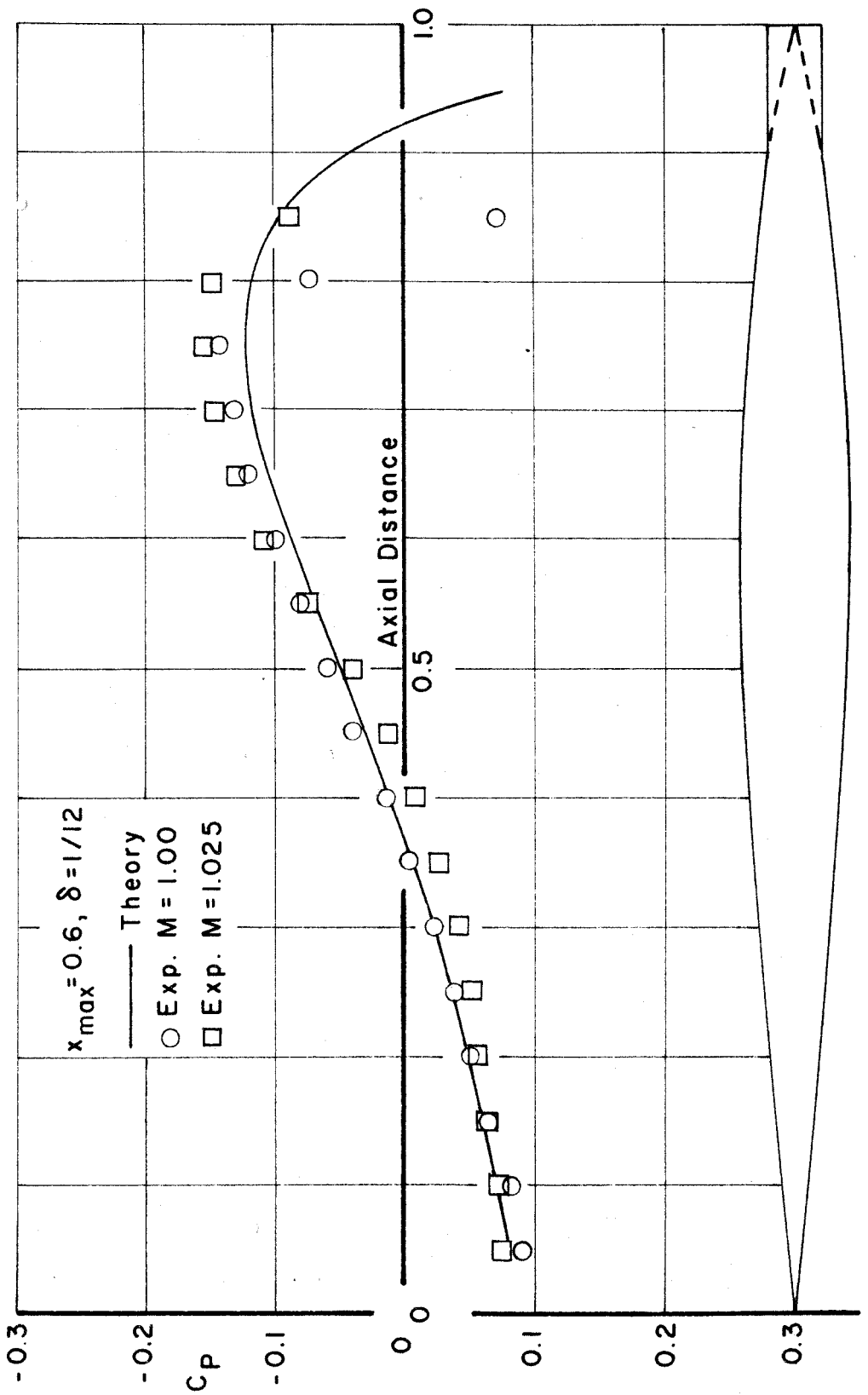

FIG.6 SLENDER BODY PRESSURE DISTRIBUTION

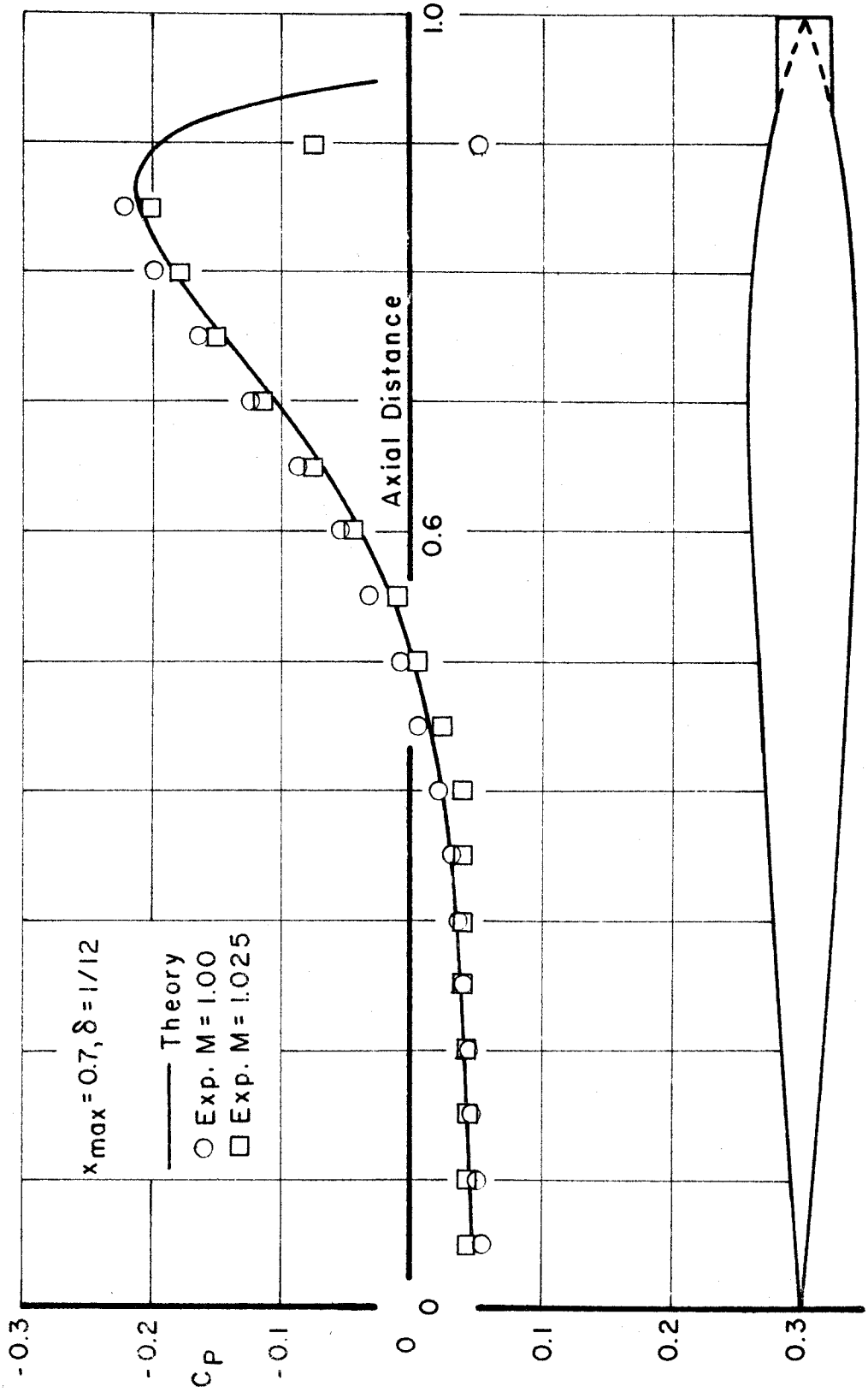

FIG.7 SLENDER BODY PRESSURE DISTRIBUTION

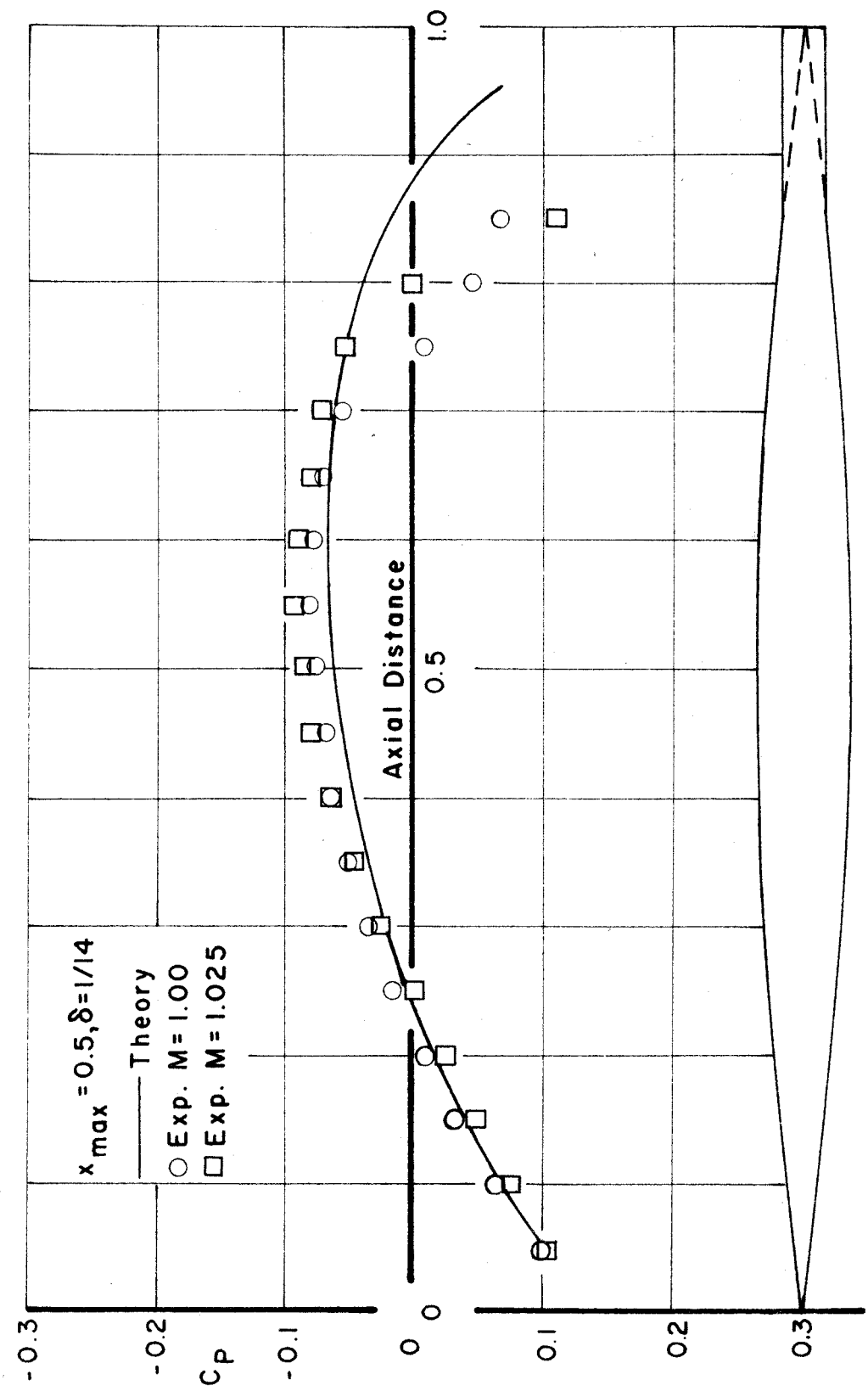

FIG.8 SLENDER BODY PRESSURE DISTRIBUTION

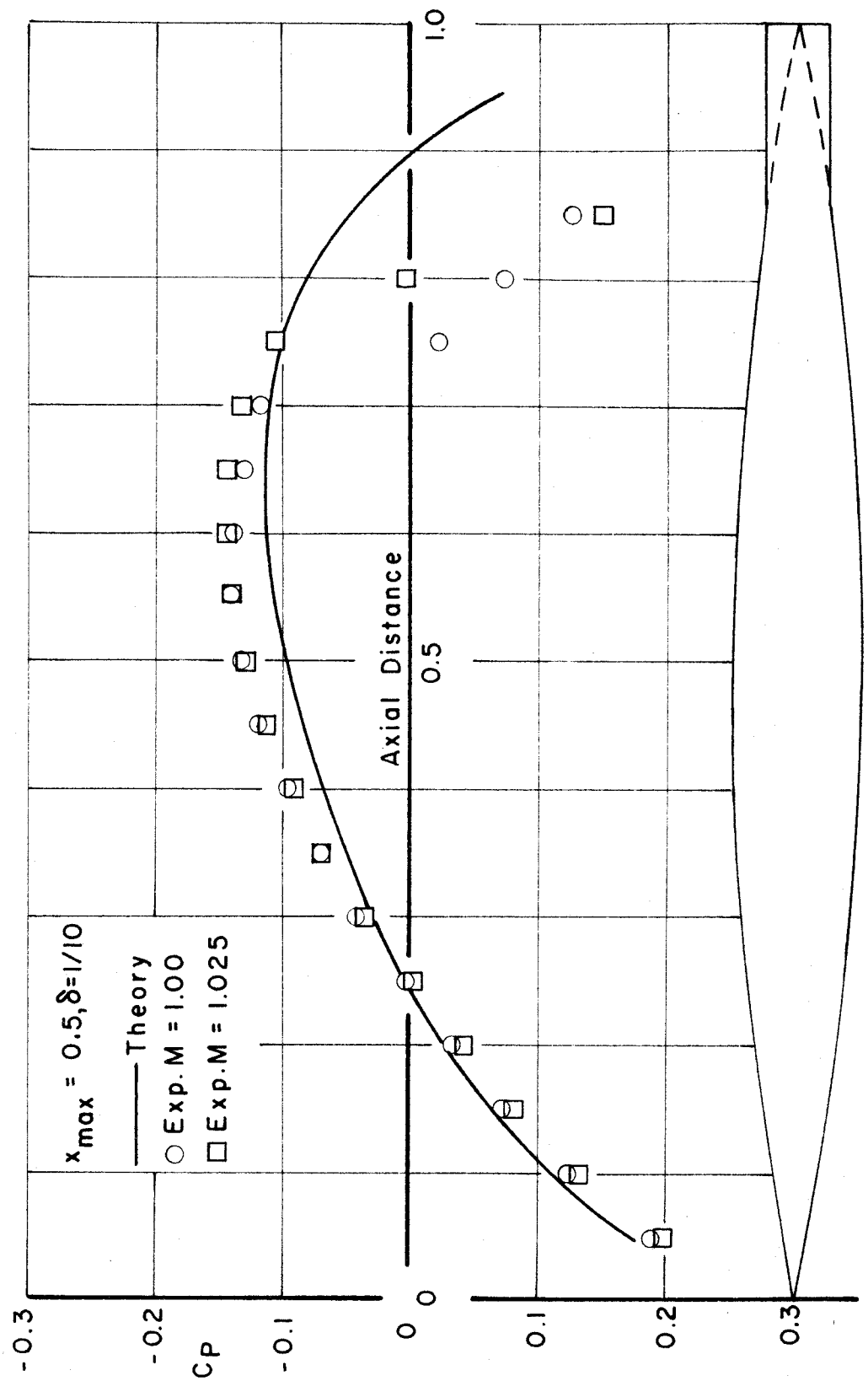

FIG. 9 SLENDER BODY PRESSURE DISTRIBUTION

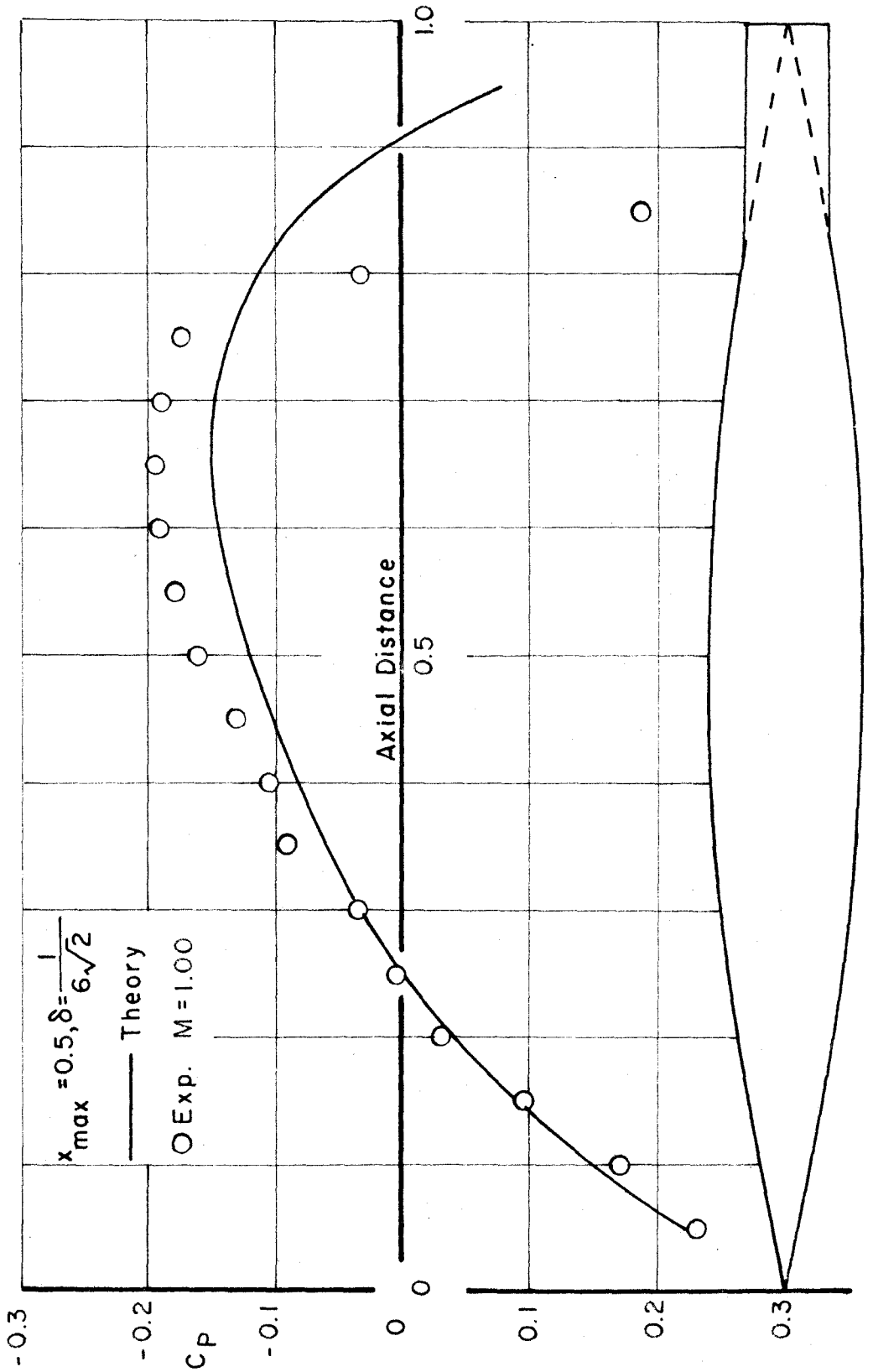

FIG. 10 SLENDER BODY PRESSURE DISTRIBUTION

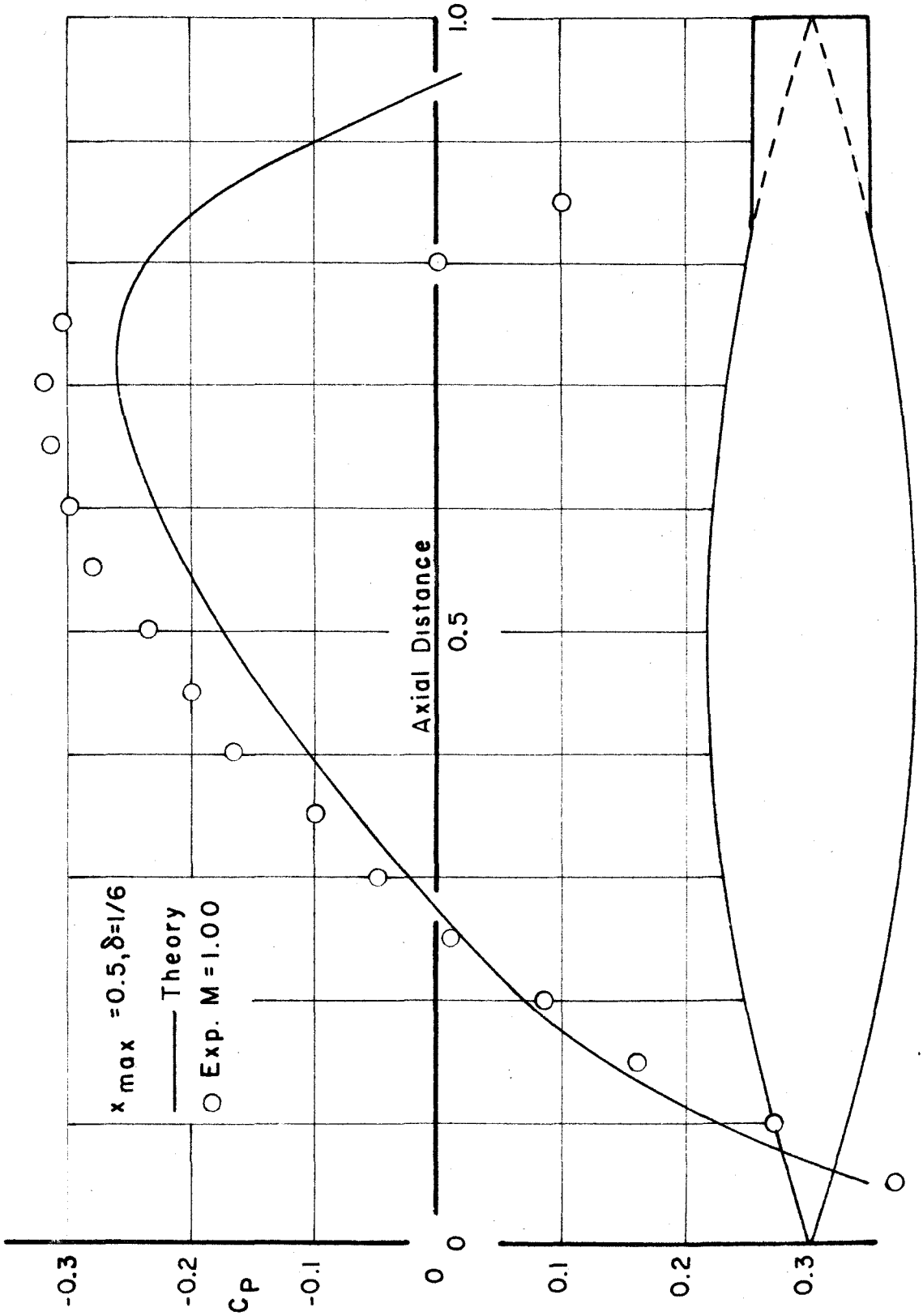

FIG.11 SLENDER BODY PRESSURE DISTRIBUTION

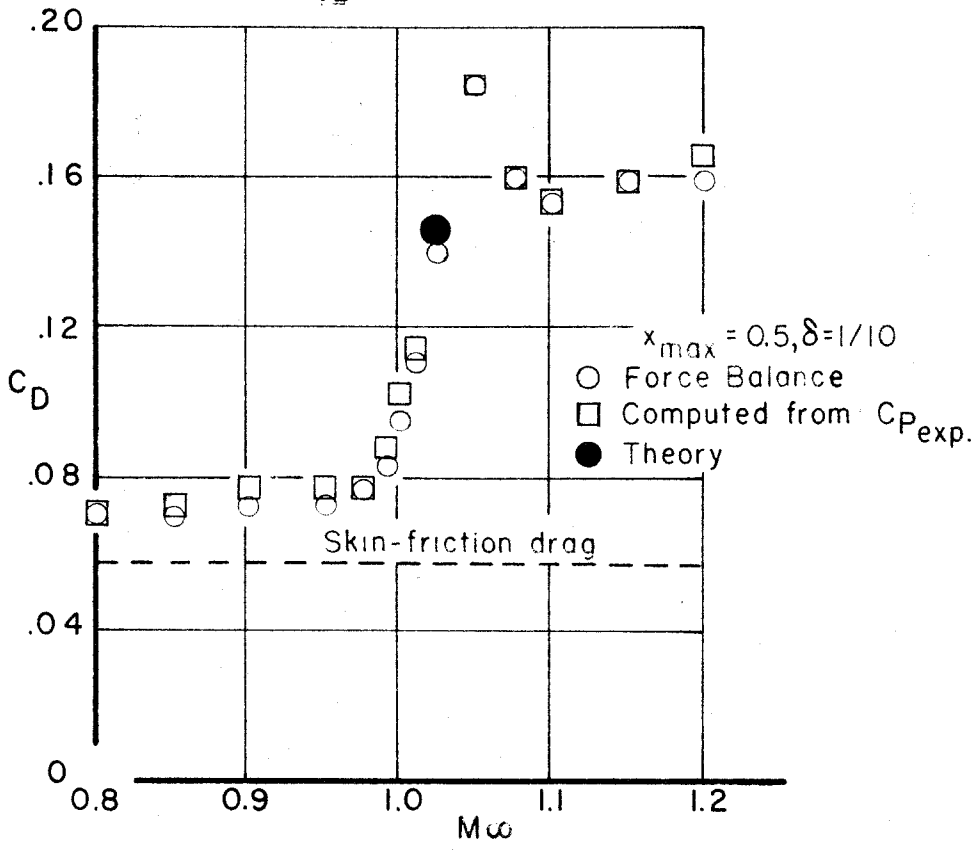

FIG.12

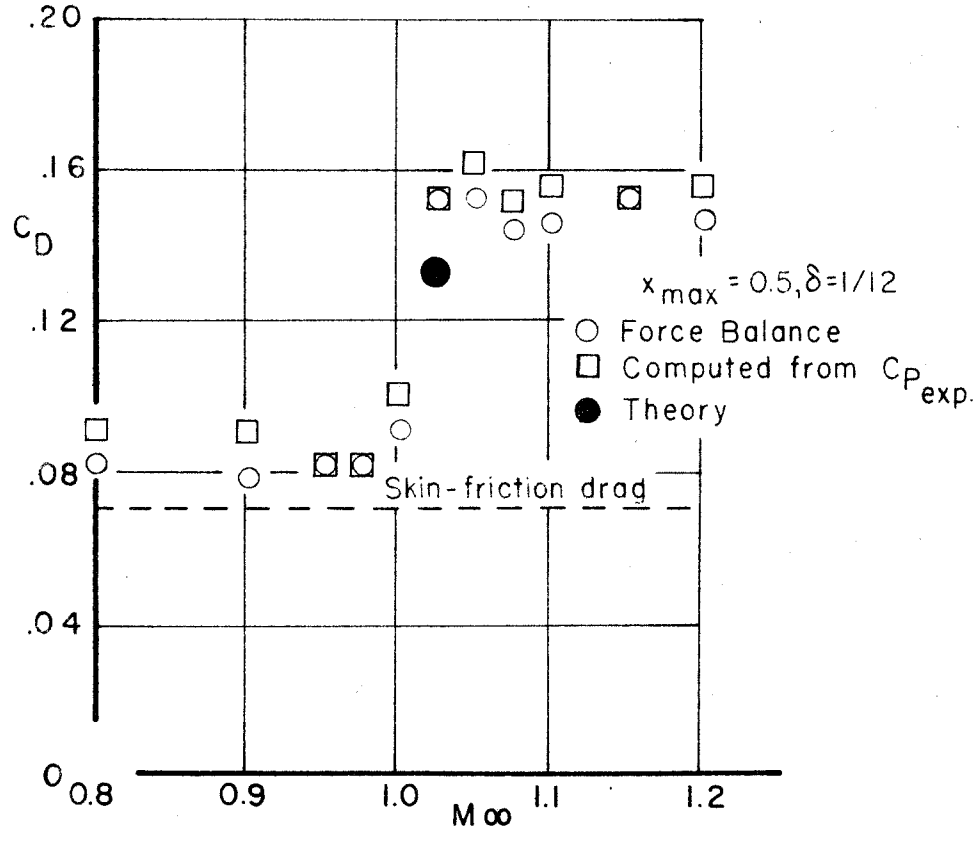

FIG.13 DRAG COEFFICIENT VS. FREESTREAM MACH NUMBER

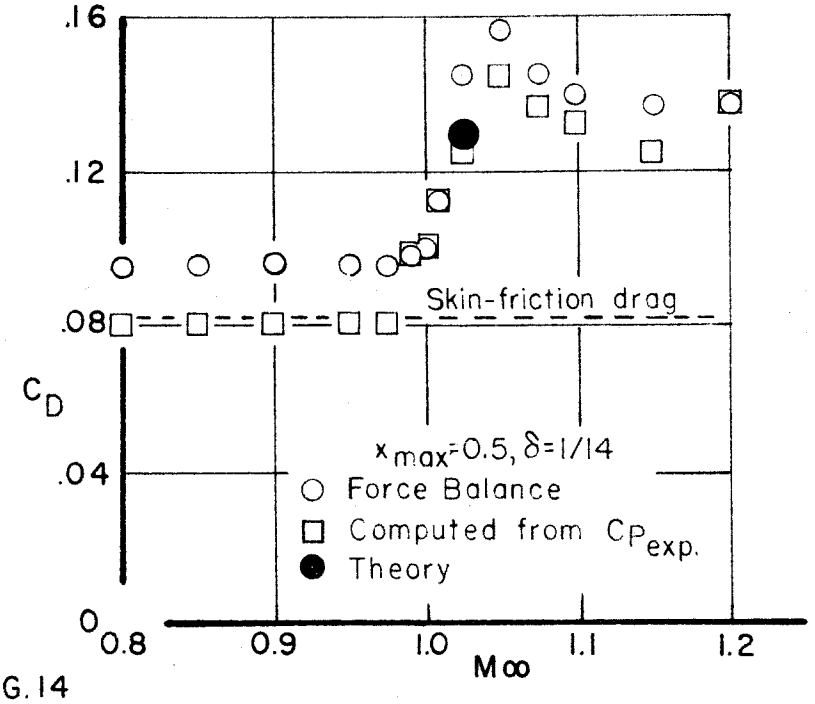

FIG. 14

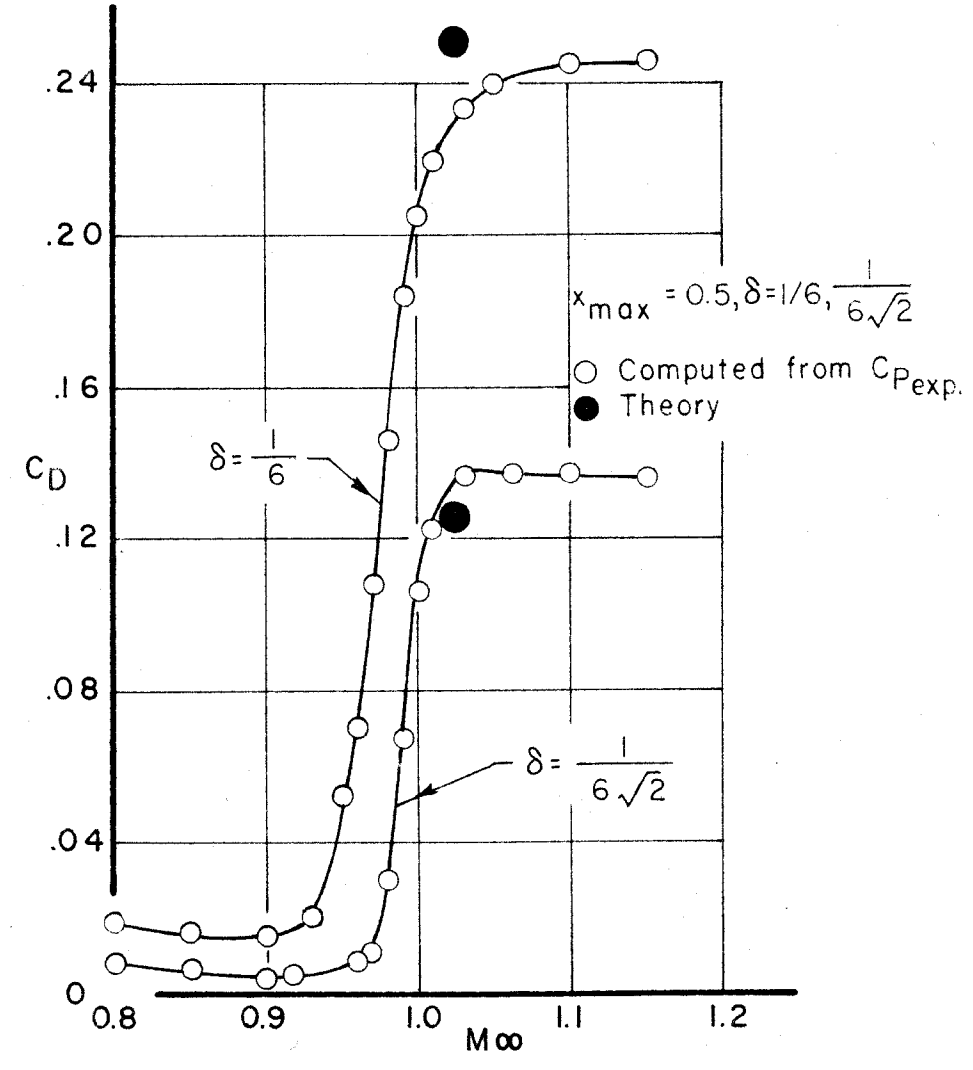

FIG. 15 DRAG COEFFICIENT VS. FREESTREAM MACH NUMBER

6. NOTATION

Some of the symbols have been used in several different contexts. In this event reference is made to the first page where each different meaning is best illustrated.

A - arbitrary constant

A_{max} - maximum cross-sectional area

a - axial acceleration constant

as used by Oswatitsch and Keune, p. 5

for sonic velocity case, p. 14

for extended transonic case, p. 31

constant in integration formula, p. 42

B - arbitrary constant

b - constant in integration formula

C - arbitrary constant

C_0, C_1 - integration constants, p. 57

C_1, C_2 - characteristics constants, p. 15

C_D - drag coefficient based on maximum cross-sectional area

C_p - pressure coefficient based on free stream conditions

c - constant in body geometry equation, p. 35

constant in integration formula, p. 42

D - drag, p. 11

arbitrary constant, p. 19

e - base of natural logarithms

F - to denote functional form, p. 7

body shape function, p. 10

hypergeometric function, p. 43

f_P - Poisson term in parabolic equation of Spreiter and Alksne

$f(\eta)$ - general function, p. 56

$f(x)$ - general function, p. 11

$f(r)$ - general function, p. 16

$\mathfrak{f}(\omega)$ - Hankel transform of $f(r)$

$g(x)$ - general function

$H(z)$ - Heaviside function, p. 56

$H_1^{(1)}, H_1^{(2)}$ - Hankel functions of the first and second kind

h - half-tunnel height

I_0, I_1 - Bessel functions of imaginary argument of the first kind, p. 19

I_1, I_2, I_3, I_4 - shorthand notation for integrals, p. 58

$\mathfrak{Im}$ - imaginary

i - $\sqrt{-1}$

J_0, J_1 - Bessel functions of the first kind

K_0, K_1 - Bessel functions of imaginary argument of the second kind

$\log$ - natural logarithm

M_∞ - free stream Mach number

M_{local} - local Mach number

M_{WT} - measured Mach number in wind tunnel

ΔM - Mach number increment between measured Mach number in wind tunnel and equivalent free flight Mach number

n - constant in body geometry equation

$\mathcal{O}$ - order of

q_∞ - free stream dynamic pressure

R - $|\omega|$

$\mathfrak{Rl}$ - real

r - radial coordinate ($r=0$ at body axis)

$\bar{r}$ - body radius distribution

r^* - radial coordinate of sonic point on body surface

$S(x)$ - source strength distribution

$T(z)$ - source strength distribution in transformed coordinates

t - integration variable in integration formula

U - free stream velocity

u - dimensionless axial velocity component

v - dimensionless radial velocty component

W - Wronskian

X - $\frac{a^2+b^2+c^2}{2bc}$

x - axial coordinate ($x=0$ at body nose, $x=1$ at body trailing edge)

$\bar{x}$ - axial coordinate where $S'(x)=0$

x_{max} - axial location of maximum cross-sectional area

x^* - axial coordinate of sonic point on body surface

Y_0, Y_1 - Bessel functions of the second kind

y - general independent variable

z - transformed axial coordinate ($z=0$ AT $x=\bar{x}$)

z_0 - nose point in transformed coordinates

z_1 - trailing edge point in transformed coordinates

Γ - Gamma function

γ - gas constant (ratio of specific heats)

δ - ratio of body thickness to length, p. 10

delta function, p. 16

positive acute angle specified in limits on Θ , p. 39

ε - small increment in axial coordinate

η - $\frac{a^2 r^2}{4z}$

θ - $\arg \omega$, p. 39

integration variable, p. 46

λ_E - axial velocity constant, elliptic case

λ_H - axial velocity constant, hyperbolic case

λ_P - axial acceleration constant, parabolic case

μ - index in integration formula

ν - index in integration formula

ξ - axial coordinate of source

ρ - $|\omega|$

ϕ - velocity potential

complete potential, p. 10, 25

incomplete potential, p. 21

for a unit-strength source, p. 18, 20

ϕ_E - unit-strength potential for an elliptic source

ϕ_H - unit-strength potential for a hyperbolic source

ϕ_{sing} - singular part of incomplete potential

$\tilde{\phi}$ - Hankel transform of potential

ω - Hankel transform variable

REFERENCES

1. Cole, J. D., and Messiter, A. F.: Expansion Procedures and Similarity Laws for Transonic Flow. Zeitschrift für Angewandte Mathematik und Physik, Vol. VIII, pp. 1-25 (1957).

2. Oswatitsch, K., and Keune, F.: The Flow Around Bodies of Revolution at Mach Number 1. Proceedings of the Conference on High-Speed Aeronautics, Polytechnic Institute of Brooklyn, pp. 113-131 (1955).

3. Spreiter, John R., and Alksne, Alberta Y.: Aerodynamics of Wings and Bodies at Mach Number One. Paper presented at the Third U. S. National Congress of Applied Mechanics, Providence, R. I., June 1958.

4. Spreiter, John R., and Alksne, Alberta Y.: Thin Airfoil Theory Based on Approximate Solution of the Transonic Flow Equation. NACA Rep. 1359 (1958).

5. Spreiter, John R.: Aerodynamics of Wings and Bodies at Transonic Speeds. Paper presented at the Eighth Japan National Congress for Theoretical and Applied Mechanics, Tokyo, Japan, September 1959.

6. Spreiter, John R., and Alksne, Alberta Y.: Slender-Body Theory Based on Approximate Solution of the Transonic Flow Equation. NASA Rep. 2 (1958).

7. Drougge, Georg: Some Measurements on Bodies of Revolution at Transonic Speeds. Actes, IX[e] Congrès International de Mécanique Appliquée, Tome II, pp. 70-77 (1957).

8. McDevitt, John B., and Taylor, Robert A.: Pressure Distributions at Transonic Speeds for Slender Bodies Having Various Axial Locations of Maximum Diameter. NACA TN 4280 (1958).

9. Taylor, Robert A., and McDevitt, John B.: Pressure Distributions at Transonic Speeds for Parabolic-Arc Bodies of Revolution having Fineness Ratios of 10, 12, and 14. NACA TN 4234 (1958).

10. Page, William A.: Experimental Study of the Equivalence of Transonic Flow about a Slender Cone-Cylinder of Circular and Elliptic Cross Section. NACA TN 4233 (1958).

11. Ward, G. N.: Linearized Theory of Steady High-Speed Flow. Cambridge University Press, (1955).

12. Watson, G. N.: Theory of Bessel Functions, Second Edition. Cambridge University Press, (1944).

13. Whittaker, E. T., and Watson, G. N.: A Course of Modern Analysis, Fourth Edition. Cambridge University Press, (1927).

14. Magnus, Wilhelm, and Oberhettinger, Fritz: Special Functions of Mathematical Physics. Chelsea, New York (1949).